DANMARKS OG GRØNLANDS GEOLOGISKE UNDERSØGELSE RAPPORT 2018/23

Architeture and mineral potential of the Paleoproterozoic Karrat Group, West Greeland

Results of the 2017 season

Diogo Rosa, Stefan Bernstein, Michelle DeWolfe, Annika Dziggel,
John Grocott, Pierpaolo Guarnieri, Jochen Kolb,
Camille A. Partin, Erik Vest Sørensen
& Robert Zimmermann

GEOLOGICAL SURVEY OF DENMARK AND GREENLAND
DANISH MINISTRY OF ENERGY, UTILITIES AND CLIMATE

GEUS

DANMARKS OG GRØNLANDS GEOLOGISKE UNDERSØGELSE RAPPORT 2018/23

Architecture and mineral potential of the Paleoproterozoic Karrat Group, West Greeland

Results of the 2017 Season

Diogo Rosa, Stefan Bernstein, Michelle DeWolfe, Annika Dziggel, John Grocott, Pierpaolo Guarnieri, Jochen Kolb, Camille A. Partin, Erik Vest Sørensen & Robert Zimmermann

GEOLOGICAL SURVEY OF DENMARK AND GREENLAND
DANISH MINISTRY OF ENERGY, UTILITIES AND CLIMATE

GEUS

Contents

Abstract

The main goal of the 2017 field season was to revise the geological maps of the southern area of Karrat Group exposures. This revision will encompass the 1:100 000 sheets of Maarmorilik 71V.2 Syd, Nuugaatsiaq 71V.2 Nord, Pannertooq 72V.2 Syd, and Svartenhuk 71V.1 Nord, originally compiled between 1980 and 1991. This third field season followed up on fieldwork carried out in 2015 and 2016 and, as the other two field seasons, was jointly financed by the Geological Survey of Denmark and Greenland (GEUS) and the Ministry of Mineral Resources of Greenland (MMR).

Within this framework, and since the focus of the first two seasons had been on the Paleoproterozoic Karrat Group, the 2017 fieldwork targeted Archean rocks, namely in Pannertooq (head of Ukkusissat Fjord), Upernivik Ø, Kigarsima/Tornit and the area south of Maarmorilik. This work led to the identification, in what was originally mapped as Archean orthogneiss, of significant paragneiss and quartzite sequences, of uncertain age. These supracrustal sequences often appear infolded with Archean orthogneiss, so some of them could possibly be unrelated to the stratigraphy of the Karrat Group. Similar infolding observed in the Qeqertarssuaq Formation, mapped in Kangilleq Fjord, suggests that this formation could possibly also be unrelated to the Karrat Group, as traditionally defined. Corroborating this interpretation is the fact that higher-P metamorphic assemblages, evidenced by garnet amphibolite and kyanite micaschist, were documented in the Qeqertarssuaq Formation, but not in overlying formations. This contrasting metamorphic evolution can be interpreted as evidence for an early thermal event, prior to Qaarsukassak Formation deposition. Alternatively, the disparate metamorphic conditions could be accounted for by juxtaposition of different tectonic units during the Rinkian orogeny. To further constrain the depositional ages of the paragneiss and quartzite (including those of the Qeqertarssuaq Formation), follow up detrital zircon geochronology is warranted. However, regardless of what the subsequent analytical work reveals, these findings appear to already imply significant revisions to the existing maps.

Within the Paleoproterozoic volcano-sedimentary succession, fieldwork allowed for the identification of the presence of the Qaarsukassak Formation (informal) in Kussinersuaq (Umiammakku Isbræ), Rinks Isbræ, Qingaarssuaq (Kangerlussuaq Fjord), Kigarsima/Tornit (Kangerluarsuk Fjord) and Kangerluarsuup Sermia. This formation hosts the stratabound mineralisation in the Rio Tinto Zinc (RTZ) Discovery area (Kangerluarsuk Fjord), where it was first defined. While no primary Zn mineralisation was observed at the defined localities, with only faint zinc zap responses obtained at Kussinersuaq, and other localities not tested for mineralisation, these findings significantly stretch the areal extent of the stratabound Zn-hosting Qaarsukassak Formation, and are therefore of economic significance. Detailed follow up photogeological mapping and interpretation of hyperspectral scenes of this mineralisation host should consequently be carried out. Further work within the Paleoproterozoic Karrat Group, included the study of the mafic volcanic rocks of the Kangilleq Fm (informal), was aimed at recognising horizons with distinct geochemical signatures (alkaline vs. subalkaline), as identified in samples collected in previous seasons, in order to elucidate petrogenesis of the volcanic rocks.

The structural setting and metamorphism of the Prøven Igneous Complex (PIC) is key to understanding the geological evolution of the region and its lower contacts and some internal structures were studied. This work demonstrated that the PIC comprises one or more tabular intrusions. In the west, near Upernavik, the complex was emplaced close to the basement-cover contact. Farther to the east and south, it seems to have been emplaced at a higher stratigraphic position within the Paleoproterozoic sedimentary sequence. Subsequently, the complex was displaced to the NW (north side of the PIC) and SE (south side of the PIC). Wherever it was studied, both North and South, this contact is a shear zone. The PIC contains abundant enclaves of meta-sedimentary rocks, particularly near the lower contact. The enclaves are most likely to be from a Paleoproterozoic sequence - the Karrat Group - although this assumption is unproven. In the instances where possible cross-cutting intrusive relations are found with meta-sedimentary rocks at the base of the PIC, the cross-cutting igneous rocks are late syn-tectonic biotite granite and leucogranites, rather than elements of the PIC proper. Earlier workers assumed that these late syn-tectonic granites and the PIC were part of the same magmatic event and were **both** late syn-tectonic. Our new field evidence from the northern contact of the PIC, consistent with recently published geochronology (Sanborn-Barrie et al. 2017), shows that the PIC was affected by intense fabric formation and folding and that its contacts with its host rocks, where we have seen them, are always concordant as a consequence of intense deformation. We conclude that the published interpretation that the PIC was emplaced relatively late during Rinkian orogenic evolution should be rejected (Grocott & Pulvertaft, 1990 and references therein).

Author contributions

DRO wrote the Background and Logistical Setup section, EVS+RZI wrote the Remote Sensing section, PGUA wrote the Regional Geology section, JKOL+ADZ wrote the Archean section with additional input from MDE+CAP on the Nunataq Formation. CAP+MDE+EVS wrote the Stratigraphy section, JG+ADZ wrote the Relationship between PIC and Karrat Group section, ADZ wrote the Metamorphism section, PGUA+JKOL wrote the Structural Geology section and DRO+SB wrote the Economic Geology section. All authors contributed to abstract and summary text and edited the report.

Background and logistical setup

The KarratZinc is a joint project between the Geological Survey of Denmark and Greenland (GEUS) and the Ministry of Mineral Resources of Greenland (MMR) aimed at understanding the crustal architecture, and provide an evaluation of the mineral potential, of the Paleoproterozoic Karrat Group. It will lead to the revision of the existing geological maps and the publication of new 1:100K map sheets of the southern part of the Karrat Group (Figure 1). A third field season took place in 2017 and, between July 10th and August 3rd, 2017, a total 10 of geologists conducted field work in the Upernavik and Uummannaq districts.

The ship Minna Martek (captain: Poul Christensen) was chartered to be used as base-camp, setting anchor in four different anchorages. At these anchorages (Figure 1), fuel depots where established, and teams worked from field camps or from the Minna Martek with air support from an Air Greenland chartered AS 350 B3 helicopter (pilot: Inge Fast).
On helicopter pilot rest days, Minna Martek was also used to sail along fjords, from which zodiacs were deployed for coastal reconnaissance mapping. The weather was good, for most of the time, with only one day of rain and snow above 400-500m.

After sailing from Nuuk with provisions, fuel and gear, the ship picked up participants in Qaarsut on the afternoon of July 10th. It subsequently sailed northwards to set up Anchorage 1, in Ukkusisssat Fjord at N 72.2676 / W 53.7611. Subsequent anchorage moves were made to Anchorage 2, in Eastern Svartenhuk (same as Anchorage 3 in 2015) at N 71.7586 / W 53.8529; to Anchorage 3, in Kangerluarssuk (same as Anchorage 1 in 2015, and Anchorage 7 in 2016) at N71.2908 / W 51.7710; and finally Anchorage 4, in Maarmorilik (same as Anchorage 8 in 2016) at N 71.1249 / W 51.2728. Anchorage moves were done on July 16th, July 23rd and July 29th, respectively.

The selection of anchorages used was constrained by the fact that an anchorage site at Niaqornakavsak, in NE Qeqertarssuaq Island, used in previous seasons, was considered unsafe, following the landslide, and ensuing tsunami, that took place in Kangilleq Fjord on June 17th. An alternative anchorage site in Inngia Fjord, near Puallarsiiviup Qooruua, was attempted, but the fjord had plenty of ice and there was no suitable place for the helicopter to land. As a result, many localities had to be reached with the helicopter, from further away than planned, out of Anchorages 2 and 3. This challenged the operations, resulting in less helicopter support and longer stops for all participants, but the key localities were visited.

At the end of the season the ship sailed with gear, leftover fuel and samples, to Nuuk, where it arrived on August 5th.

In the following sections, organised by different disciplines, the preliminary observations and results of the 2017 fieldwork are reported, which build on those acquired from the 2015 and 2016 field seasons.

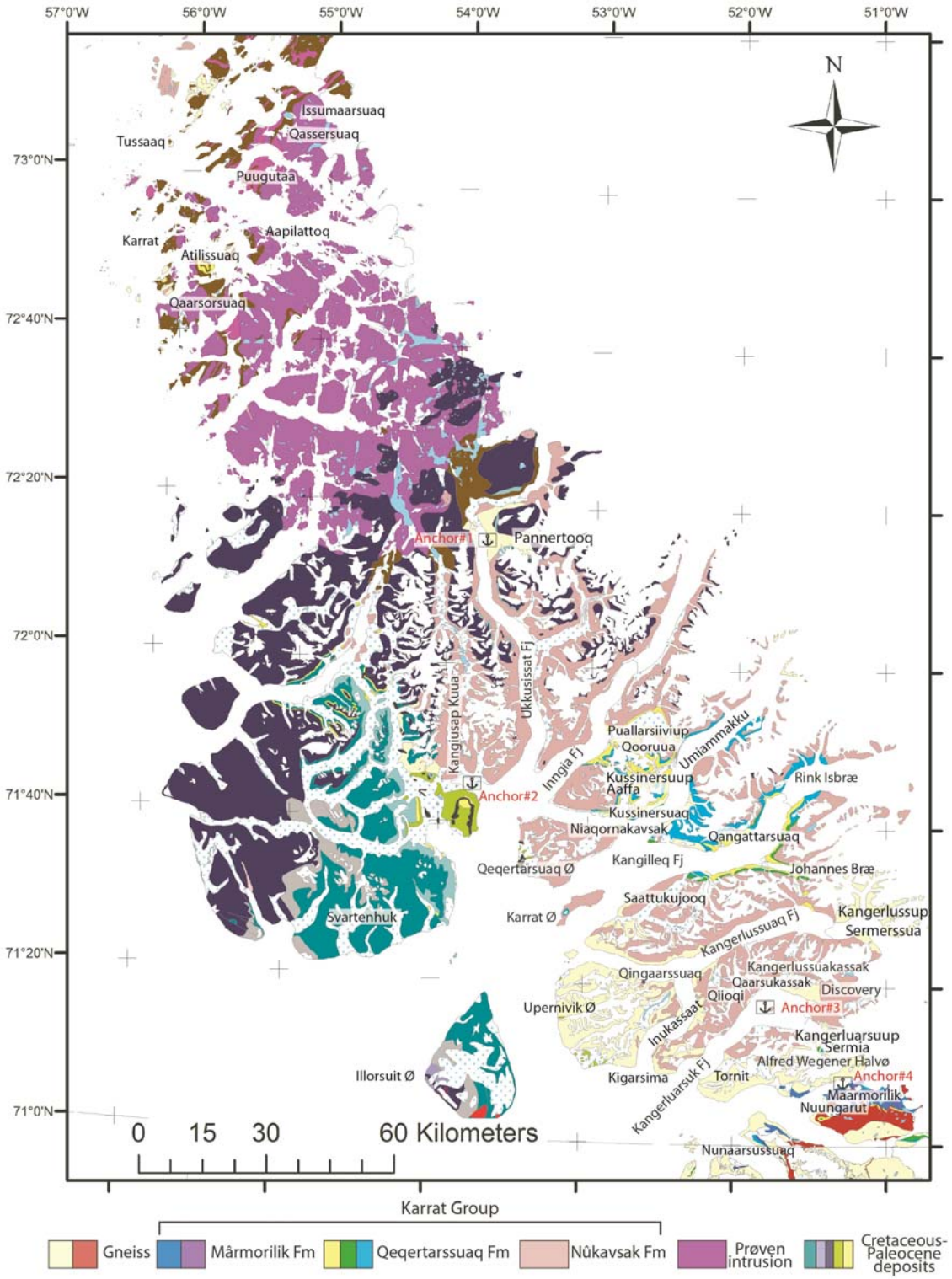

Figure 1. *Geological map of the study area (after Escher, 1980), showing anchorages in red, and highlighting localities discussed in the text.*

Remote sensing

Oblique aerial photography (photoflying)

The study area is characterised by steep alpine terrain that in many places is completely inaccessible. This makes field work an extremely difficult task. In 2015 and 2016, in order to successfully overcome these obstacles, a strategy involving acquisition of oblique stereo-images that can be used for 3D-mapping, interpretation purposes and topography extraction was deployed. The result was a dataset that covers large parts of the field area. In 2017, new oblique stereo-images were acquired as supplement to the existing dataset. Around 3400 new oblique stereo-images were collected from the Pannertooq area (Figure 2), Upernivik Ø, south of Johannes Bræ and the southern part of Alfred Wegener halvø (Figure 3). The stereo-images were collected from helicopter and boat using a calibrated Canon EOS 5D Mark II digital-SLR camera equipped with a 35 mm Carl Zeiss Distagon.

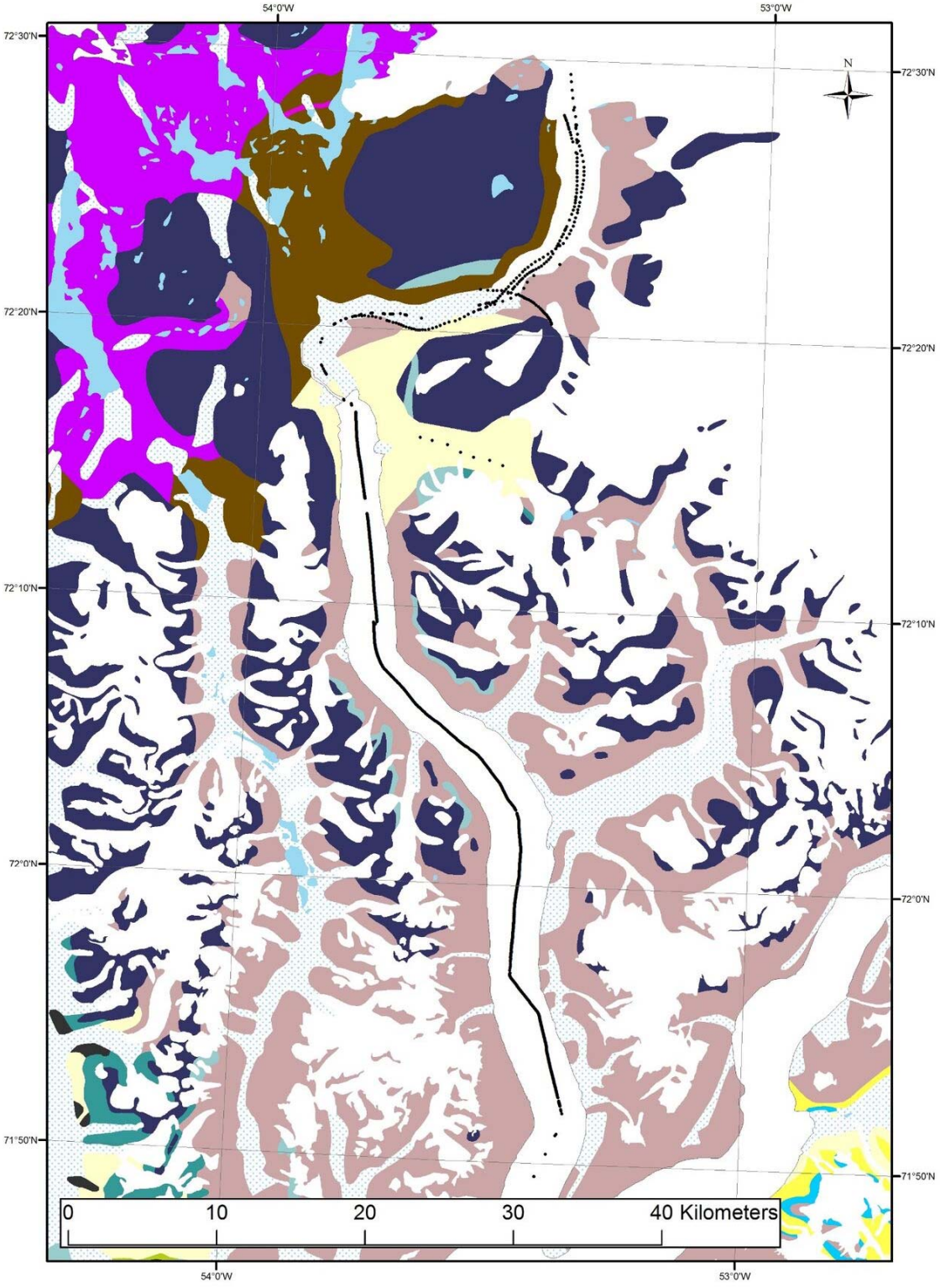

Figure 2 . *Location of collected stereo images (black lines) superimposed on geological map after Escher (1980). Same legend as in Figure 1.*

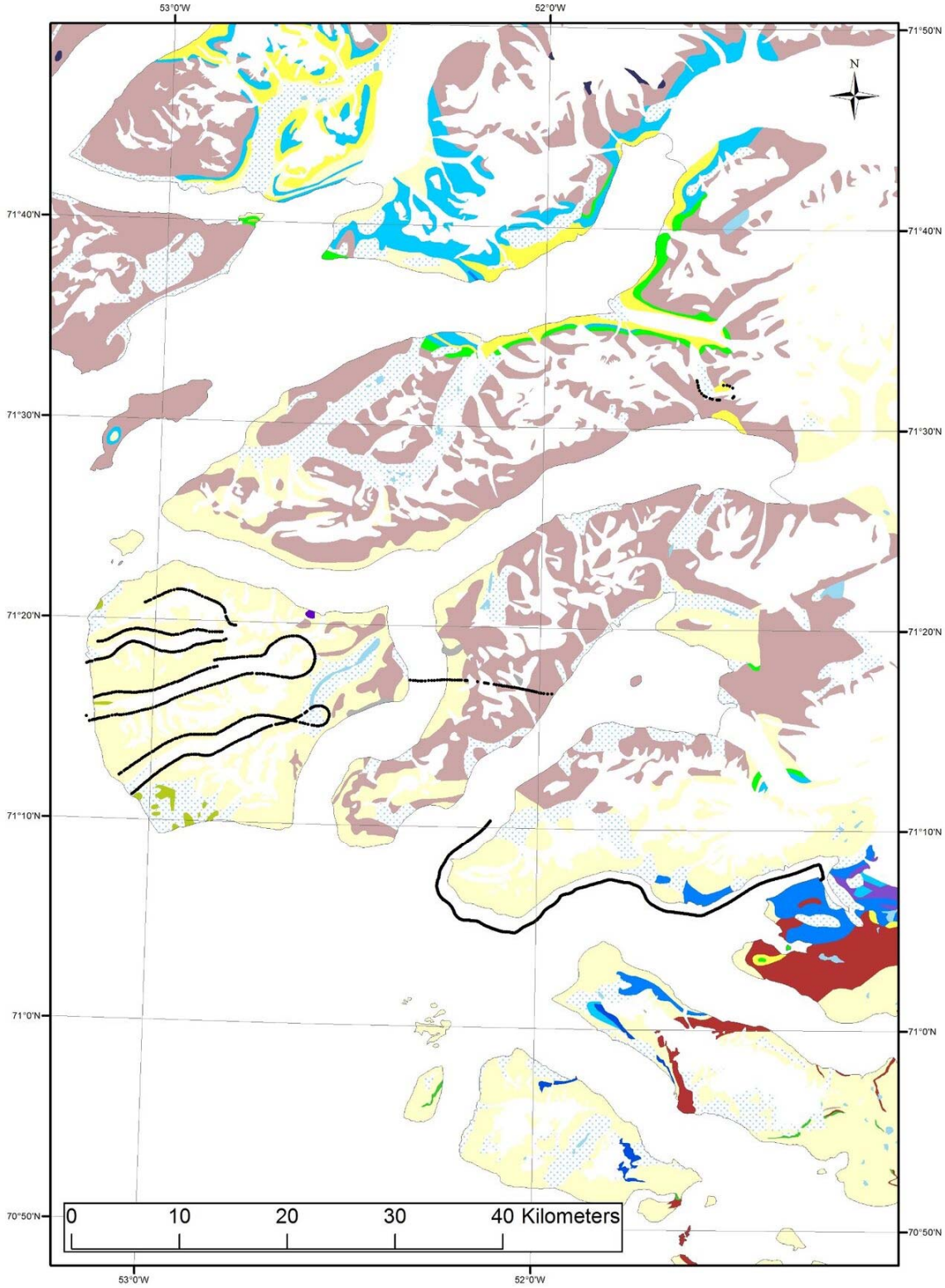

Figure 3. *Location of collected stereo images (black lines) superimposed on geological map after Escher (1980). Same legend as in Figure 1.*

Drone-borne surveys

For drone-borne data acquisition, a sensefly ebeePlus fixed-wing Unmanned Aerial System (UAS or drone) was deployed. Based on the experiences in the last two years, the use of fixed-wing UAS with dedicated sensors is recommended in Greenland. Due to long flight time, low weight and packing size, fixed-wing UAS outperform multi-copter systems. The ebeePlus (Figure 4-b) features 60 min flight time and different payload options including a 4 channel multispectral Parrot Sequoia camera. This camera was assessed during the surveys for its capability to map iron staining (gossan) as an indicator for sulfide-rich showings like VMS type deposits.

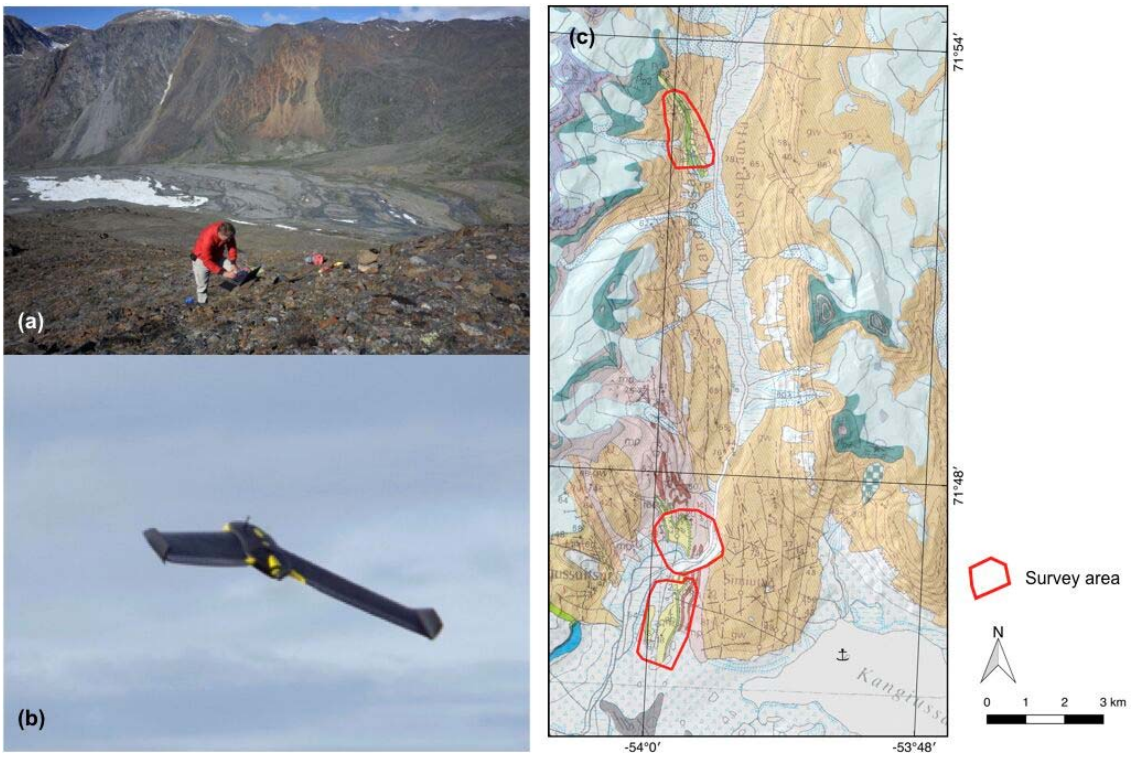

Figure 4. *UAS flights at Kangiusap Kuua: a) Base station setup with view on rusty weathered outcrops.; b) Fixed wing sensefly ebee UAS in action; c) Overview map with outlined survey areas in Kangiusap Kuua area.*

A planned UAS survey and sampling campaign at the Niaqornakavsak and Umiammakku REE showings could not be realised due to strong glacier wind (>12 m/s). Thus, UAS surveys focused on the Central (17RZI042 and 17RZI062) and Southern (17RZI043) Kangiusap Kuua VMS-type showings instead (Figure 4-c). Flight altitude was set relative to the ground elevation to achieve an average resolution (GSD) of 11 cm for the multispectral camera and with 80% horizontal and 65% vertical overlap. Drone-borne images were acquired according to predefined flight plans over the areas of interest and were geo-tagged in post-flight processing.

UAS images were used for 3D surface reconstruction via the Structure-from-Motion Multiview-Stereo (SfM-MVS) algorithm. Various derivates can be calculated therefrom, including geomorphic indices (e.g., Slope, Aspect, Topographic Position Index) or spectral mapping products (band ratios for vegetation and iron-bearing faces). Resulting 3D surface models and multispectral mosaics are interpreted for mineralisation indicators.

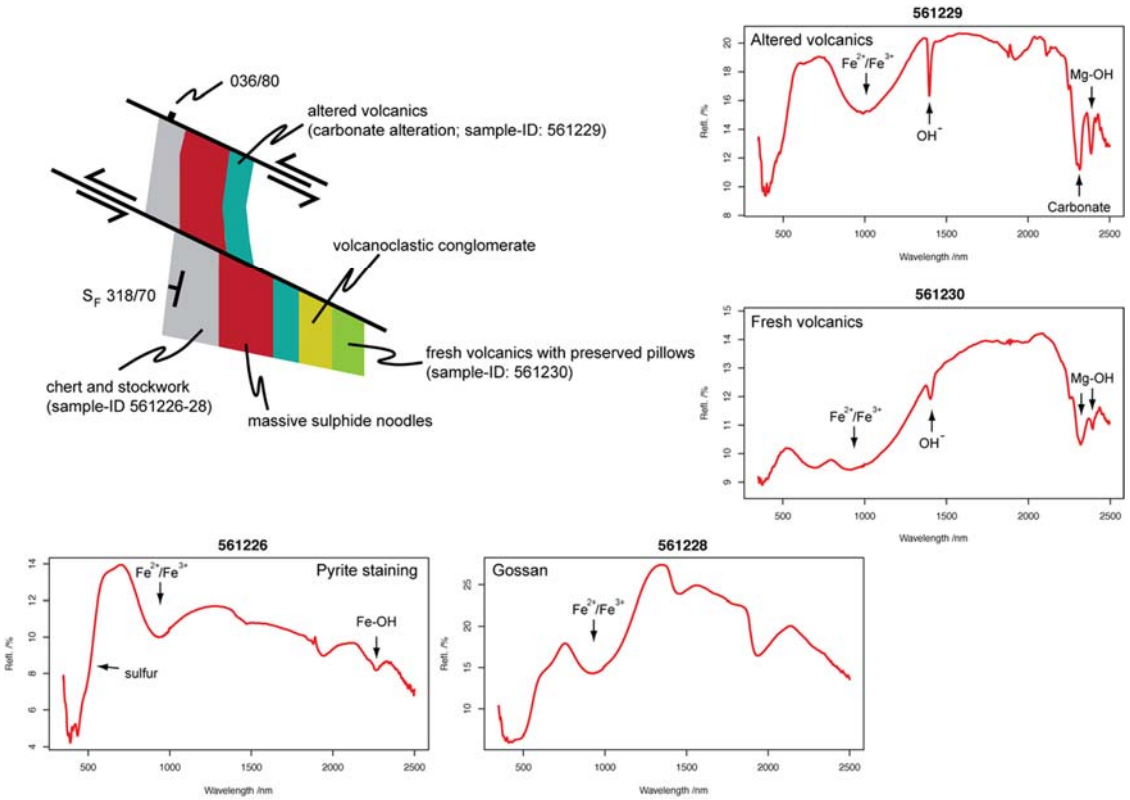

Figure 5. *Spectral signatures of selected rock units from Kangisuap Kuua. A complete VMS sequence from fresh basaltic rock with preserved pillows to chert and stockwork mineralisation is exposed. Note the increasing absorption due to Fe-charge transfer around 950 nm and the increase of the carbonate related absorption in the altered volcanics.*

In the southern part of the Central Kangisuap Kuua VMS sequence (17RZI042), selected lithologies are sampled and analysed by NIR spectroscopy (Figure 5). The samples (561226 - 561230) represent a complete profile across the sequence of fresh basalt with preserved pillows, carbonate-altered basalts and black cherty cap rock with stockwork, pyrite staining and a small gossaneous cap. The increasing degree of alteration is overall well visible with depth-increase of the iron absorption around 950 nm. Further, the spectra prove the carbonatisation of the basalt during hydrothermal alteration as documented by the deep absorptions for crystal-water, carbonate and Mg-OH and an increase of the iron absorption.

The shape of the spectra and location of characteristic absorption can now be used for mineral mapping via the drone-borne multispectral data using a simple band ratio for iron minerals (B1/B4). However, the resulting map still shows many false positives due to debris and sediment. Previous studies in Australia or Namibia show a distinct correlation between gossans and positive topographic features. Thus, a combined approach of multiplying the band ratio with the Topographic Position Index (10m filter width) and subsequent threshold-ing is applied (Figure 6) to map the gossan. This result can be combined with structural interpretations, e.g., to trace foliation and fault displacements.

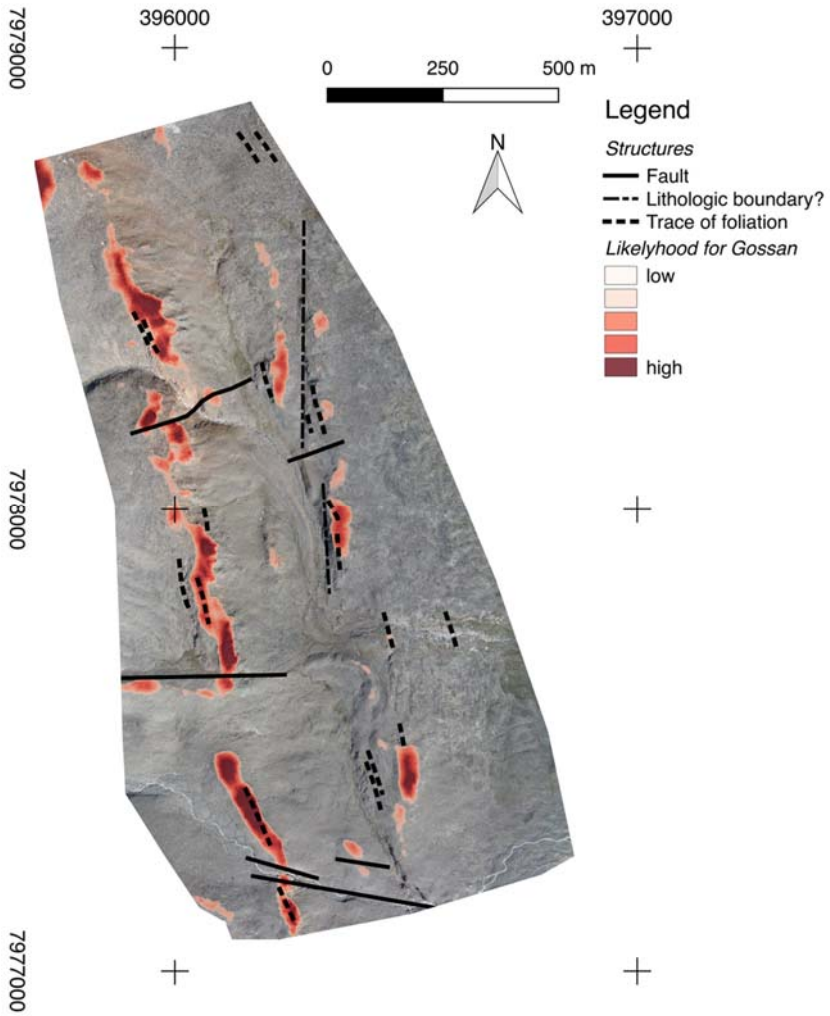

Figure 6. *Likelihood for gossan at Central Kangisuap Kuua draped on an orthomosaic of the area. Overlain are structures inferred from orthomosaic. Dark red indicates a high probability for gossan and thus should be focused for sampling.*

Hyperspectral Imaging

While sailing into the Ukkusissat Fjord, hyperspectral scenes of the East facing walls (Western coast) were gathered with a boat-based hyperspectral imaging setup starting at 4.00 am in the morning until reaching Anchorage #1 around 9.00 am. Due to morning light and low sun elevation, the illumination of the first hyperspectral scenes is not optimal. However, the dyke complex exposed in the northern part of the fjord is in good data quality. Selected points were visited during a follow up coastal reconnaissance on July 16 while moving anchorage to #2.

To get a continuous hyperspectral profile from the Nûkavsak Formation (southern part of Ukkusissat Fjord) towards the Prøven Igneous Complex, two additional scenes were taken from location 17RZI004 and 17RZI007 respectively towards West on Jul 11, 2017. However, due to gentle topography, the imaging geometry from 17RZI007 is not optimal. Further, vegetation cover increases with smoother topography. The coverage of HSI scenes is shown in Figure 7. For every scene, GPS location of the HSI instrument and view direction was protocolled.

A compact Specim AisaFenix hyperspectral camera was used for data acquisition. It is a push broom HSI sensor in the wavelength range from 380 to 2500 nm. VNIR and SWIR sensors are using the same optics, which leads to a simultaneous acquisition of both sensors and storage in one file with same sensor/image resolution. Pre-processing from raw data to at-sensor radiance is done with a dedicated script. All scenes are pre-processed until step (5) including following protocol:

(1) dark current subtraction
(2) normalisation of data
(3) multiplication of sensor calibration file
(4) radiometric rescaling
(5) Geometric correction with a defined Look-up table (file ending *_CAL_GLTX.*)

These steps can be followed by a conversion to reflectance using empirical line calibration or similar approaches and spectral smoothing. Atmospheric features by upwelling water vapour and movements of the boat during image acquisitions demonstrate the need for problem specific corrections. Those are presented by Salehi et al. (2018) and Lorenz et al. (2018) and should be applied prior to further analysis. The steps include:

(6) wave-correction assuming the coastline as a straight line, (when processing a boat based scan, Salehi et al., 2018) and

(7) atmospheric correction by removal of water vapour related absorption (as described in Lorenz et al., 2018)

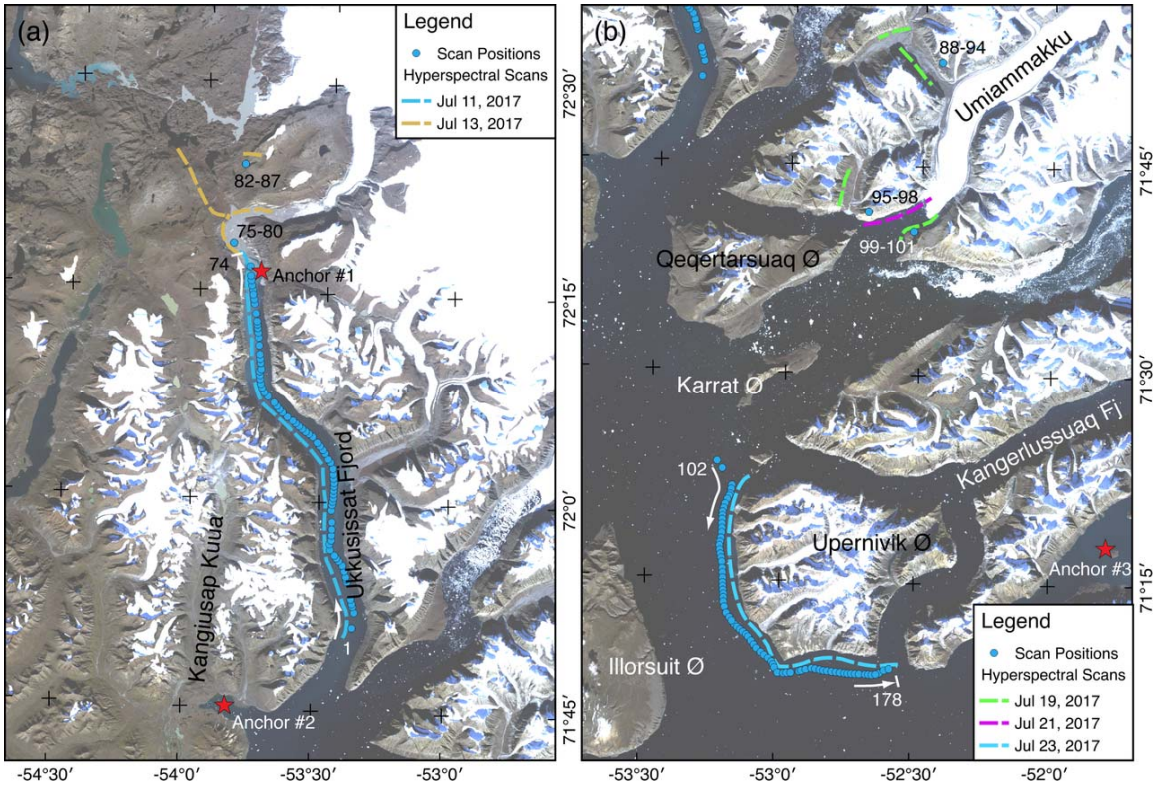

Figure 7. *Coverage of hyperspectral scenes acquired: a) while sailing in Ukkusissat Fjord (July 11, 2017); b) along the coast of Upernivik Ø (July 23, 2017) as well as with helicopter support in other days*

Work focused on developing a 3D integration workflow for hyperspectral mapping on the example of the Maarmorilik area. A simple Minimum Wavelength mapping (van der Meer et al., 2018) approach with subsequent supervised classification is applied therefore on data from 2016. The 3D integrated classification result for Black Angel Mountain follows preliminary results presented in Rosa et al. (2017) and is shown in Figure 8.

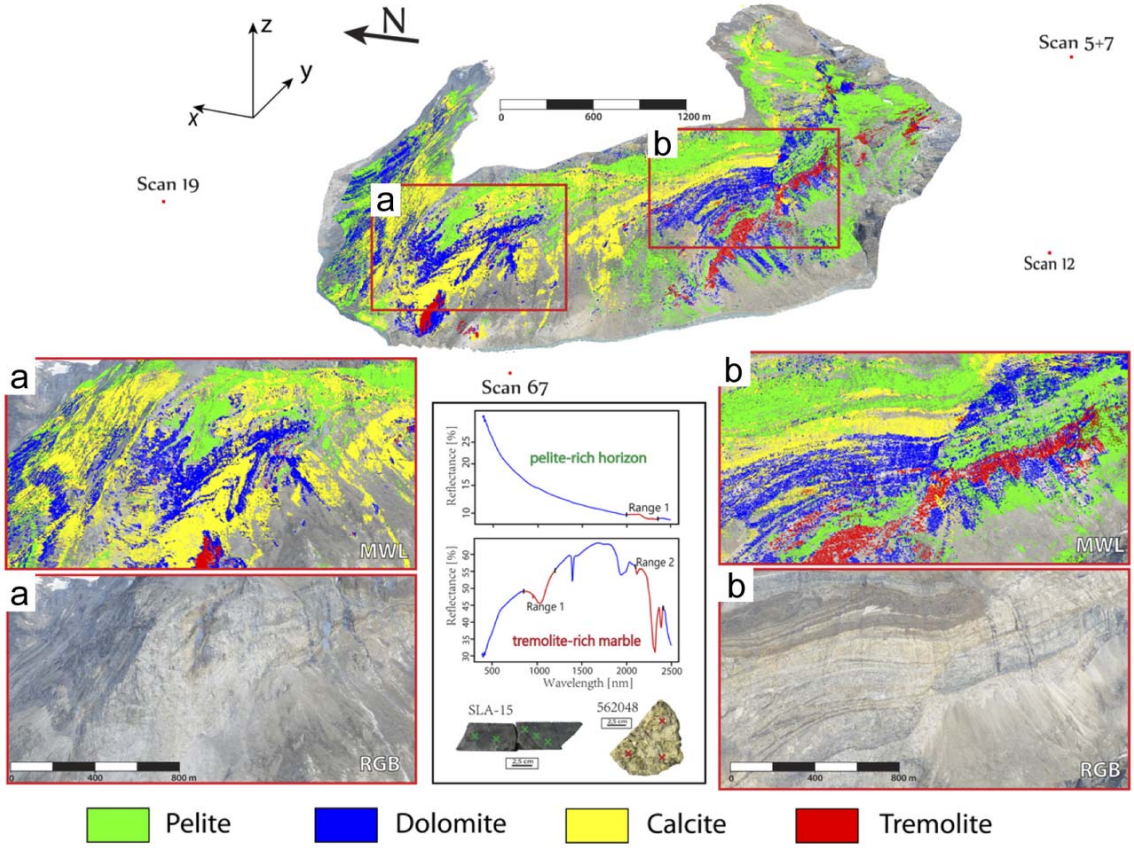

Figure 8. *Results of the 3D integrated classified hyperspectral image set for Black Angel Mountain. The two zoom-ins, highlight exemplary mineralogical information not visible in RGB. From Unger (2018).*

The difference between the lower (dolomite-dominated) and upper (calcite-dominated) Mârmorilik Formation is observable in the hyperclouds (3D hyperspectral point clouds). Different deformation geometries can be highlighted and assigned to different deformation stages (see Figure 9).

(1) One example is the calcite- and dolomite-rich folded layers of the northern Black Angel Mountain - probably assigned to isoclinal folding (Figure 9a). These tight folds are south vergent and could be correlated to D2 (see Rosa et al., 2017).

(2) Another example is the block rotation along S2 normal faults. The suggested interpretation is based on the laterally extensive dolomite-rich “block”, which occurs also on the N-facing cliff wall of the Black Angel Mountain. Thus, this block is rotated in a clockwise direction (dextral). Small thrust faults, which occur on the N- and S-facing cliff- walls, support this interpretation (as in Carmichael, 1985).

(3) At the southern end of the cliff-wall, a reverse drag along a normal fault is observed (Figure 9c). The concave appearance of the drag indicates that the normal fault has been reactivated as a thrust fault (Grasemann et al., 2005). The displacement of the normal fault is approximately 150-200 m.

(4) Within the dolomitic rich layer of the present footwall unit, a shear fold out of calcite and pelite is apparent (Figure 9d). This shear fold is related to the heterogeneous composition of the marbles of the Mârmorilik Formation. Pelite and calcite-rich (less Mg-content) marbles possess a weaker rheology than a dolomite-rich (Mg-rich) marble (Kushnir et al., 2015). Thus, during a thrusting event, the calcite and pelite rich layers formed this shear fold.

The overall formation of ductile folds and faults within the marble of the study area is the result of the metamorphism event (~450°C, 1.5 kbar) of the Rinkian Orogeny. The two major orientations of the faults within the study area are SE-NW (S1) and NNE-SSW (S2). These measurements are extracted from three-point generated surfaces of representative polylines of digitised faults.

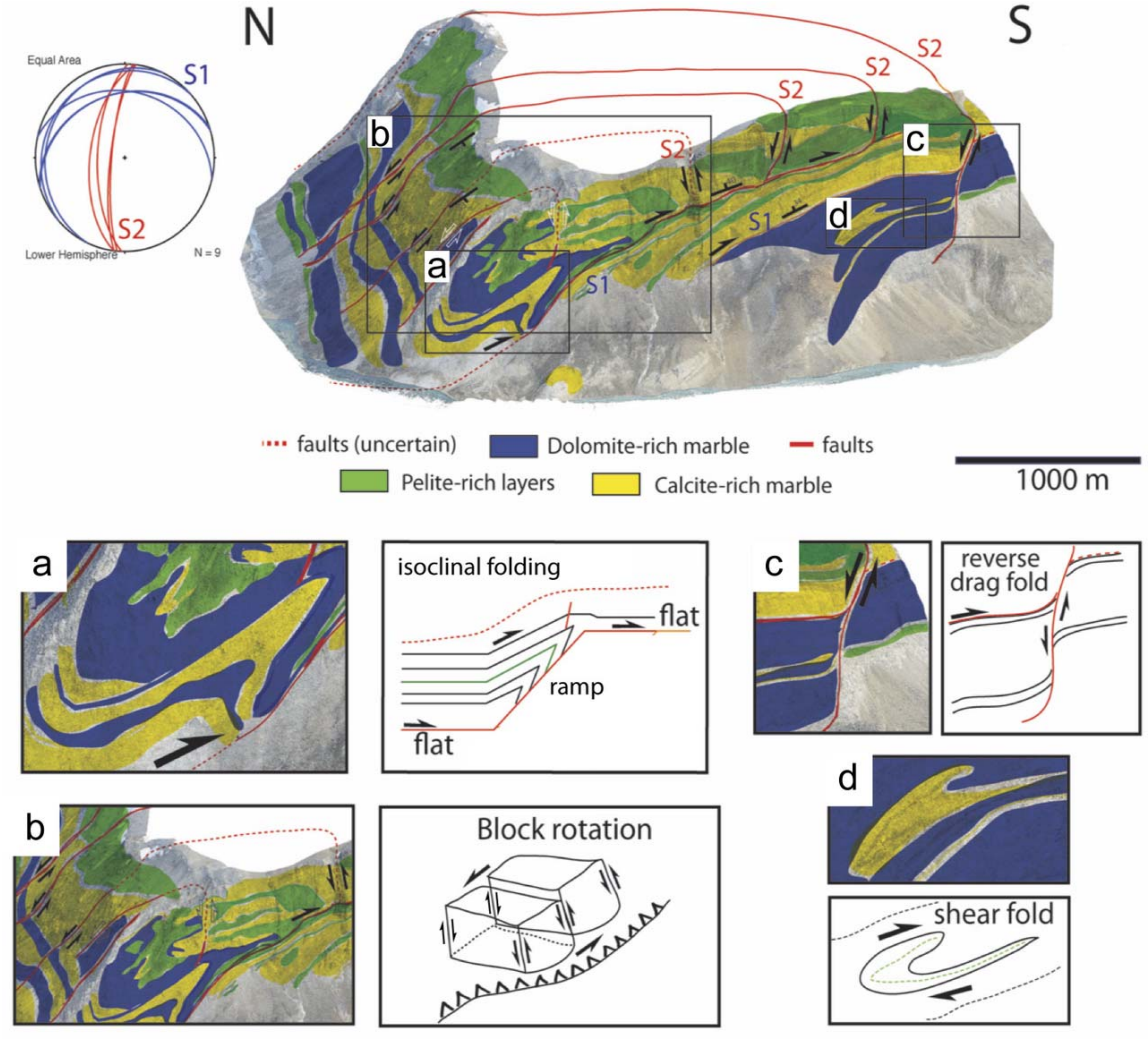

Figure 9. *Geological interpretation of Black Angel Mountain based on integrated hyperspectral data and literature (Pedersen, 1977; Garde, 1978; Carmichael, 1985). Different areas are zoomed for highlighting certain structures : a) Isoclinal folding, probably correlated to a flat-ramp geometry; b) Clockwise block rotation, resulted from oblique thrusting; c) Reverse drag along a normal fault; d) Calcitic shear fold within a dolomite rich marble. Results and figure modified from Unger (2018).*

The hyperspectral mapping results of the vertical cliff-walls show additional detailed geological and structural information compared to previously published geological maps (e.g., by Garde, 1978, or King, 1981). However, small pelite horizons cannot be detected due to the low resolution of the hyperspectral images. The resulting 3D geological map of the northern Black Angel Mountain (Figure 9) is an approximation of the hyperspectral mapping results. Related to a low signal-to-noise ratio (SNR) of the HSI 19, the mapping results and the N-facing wall of the geological map are more affected by false-positives (pixels that have been misclassified).

The hyperclouds (Unger, 2018) are validated by ground samples of a pelite-rich (SLA-15p), calcite-rich (SLA-15c), dolomite-rich (562032) and a tremolite-rich (562048) sample. These spectra are used as validation and comparison for mapping lithology within the hyperspectral images. The characteristic positions of calcite and dolomite absorption features of the HSI could be validated with reference spectra and literature (Zaini et al., 2012). Additionally, it could be proved that the presence of tremolite within dolomitic marble shifts the characteristic absorption feature to even shorter wavelengths (2310-2315 nm). The overall comparison between target and reference spectra shows a good correlation of spectral shape and feature position within the validated data. Only a small shift of the absorption features of calcite-, tremolite- and dolomite-rich pixels of the target spectra to smaller wavelengths can be observed. The shift was about to 5 nm in all hyperspectral images but is below the spectral sampling interval. In addition, all reference samples were validated by pXRF. Derived elemental compositions enable the calculation of the Ca/Mg-ratios and the classification of limestones and dolomites after Chilingar (1957). The average of sample SLA- 15c features a Ca/Mg-ratio of 172.62 ± 4.91 and would, therefore, be classified as calcitic limestone. Additionally, the averaged ratio of sample 562032 is 4.23 ± 0.78, indicating a highly dolomitic limestone. Sample 562048 is classified as a dolomite with a low averaged Ca/Mg ratio of 1.61 ± 0.12.

Regional Geology

In the study area reworked Archean gneisses are overlain by supracrustal successions of the Paleoproterozoic Karrat Group. The Karrat Group was originally defined by Henderson & Pulvertaft (1967) as comprising two formations: the Qeqertarssuaq Formation and the Nûkavsak Formation. The group was extended by Henderson & Pulvertaft (1987) to include the Mârmorilik Formation (previously considered to be of Archean age), which was deposited in a sub-basin separated from the Qeqertarssuaq Formation by a basement topographic high. They suggest that siliciclastic-dominated Qeqertarssuaq Formation in the northern sector is laterally equivalent to the carbonate-dominated Mârmorilik Formation in the south. The Karrat Group and the Archaean basement were metamorphosed and folded during the Rinkian orogeny (Henderson & Pulvertaft 1987; Grocott & Pulvertaft 1990).
During the compilation of 1:500 000 maps in West Greenland (Escher 1980) the deformation of the Precambrian terrain north of Ilulissat was separated from the Nagsugtoqidian complex and defined as the Rinkian mobile belt (Escher and Pulvertaft, 1976). The stratigraphy, structural style and age of the Precambrian metamorphic rocks of this part of West Greenland were so similar to what was described from the Foxe fold belt in central Baffin Island that the Foxe and Rinkian belts were considered to form a single tectonostratigraphic unit: the Foxe-Rinkian belt (Henderson and Pulvertaft 1987). Connelly et al. (2006) and more recently Sanborn-Barrie et al. (2017) have shown that the Nagssugtoqidian orogen and the Rinkian belt may be linked through the northern part of Disko Bugt defining a single orogen, the Nagssugtoqidian– Rinkian orogen, that they thought to be >1100 km wide and to stretch from the Nagssugtoqidian foreland in the Kangerlussuaq district far northwards into Melville Bugt. On the other hand, based on the evidence from fabrics and structures and the regional thrust transport direction, Grocott and McCaffrey (2017) suggest that the Rinkian belt does not represent a continuation of the Nagssugtoqidian orogen (as suggested by Escher and Pulvertaft, 1976), and it was not formed by north–south convergence.

In the present report, we will refer to the Rinkian belt as the Rinkian orogen and the deformation within the orogen is represented by fold-and-thrust systems.

Archean Lithologies

Archean rocks are widespread between Pannertooq, in the north, and Nunngarut, in the south, and are dominantly granitic orthogneiss. They were already recognised in early studies (Krueger 1928) and later classified as the Umanak Gneiss, which has its type locality in the Umanak Fjord (Henderson and Pulvertaft 1967). They are mainly biotite- or biotite-hornblende-bearing, granodiorite orthogneiss. Their texture varies from homogeneous to banded, with local development of lit-par-lit banding. Thin horizons and lenses of amphibolite and augengneiss are parallel to this banding (Henderson and Pulvertaft 1967). The Nunataq Formation has its type locality on a nunatak south of Maarmorilik and is mainly composed of amphibolite, hornblende schist with minor siliceous and graphitic schists, quartzite and calc-silicate rocks (Henderson and Pulvertaft 1967).

The Archean orthogneisses record different stages of deformation and metamorphism at the various sites of observation in the localities of the 2017 field season. In addition, outcrops of the Nunataq Formation were revisited.

Umanak Gneiss

At Pannertooq, at the head of Ukkusissat Fjord, the Archean orthogneiss is a grey, banded migmatite (plagioclase-quartz-bioite-(K-feldspar)) with meso-scale folds (Figure 10-a). The migmatite is crosscut by only weakly deformed pegmatite (quartz-plagioclase-K-feldspar-(garnet); Figure 10-b). Locally, up to 4 m thick and 20 m wide amphibolite lenses are observed (Figure 10-c). The amphibolite is composed of hornblende-plagioclase-quartz-biotite and has leucosomes with a plagioclase-quartz-clinopyroxene-(orthopyroxene) assemblage, indicating peak metamorphism in the upper amphibolite or granulite facies. Locally, up to 20 m wide amphibolite lenses crosscut the fabric in the migmatite, indicating that they likely represent metamorphosed mafic dykes (Figure 10-d). Hornblende of one of the crosscutting amphibolite lenses yields an Ar-Ar age of 1795 ± 3 Ma interpreted as the age of metamorphism (Sidgren et al. 2006).

Figure 10. *Pannertooq: a) Photograph of the typical Archean migmatite; b) Archean migmatite crosscut by little deformed pegmatite; c) Amphibolite lenses in migmatite; d) Amphibolite cross-cutting foliation in migmatite.*

On Svartenhuk, the orthogneiss in the northwestern part is a migmatite with local agmatitic texture (see also Grocott et al. 1987, Rosa et al. 2006). The rock is a grey gneiss with a plagioclase-K-feldspar-biotite-quartz assemblage (Figure 11-a). Amphibolite facies leucosomes are composed of plagioclase-K-feldspar-biotite-quartz-(garnet) and later crosscutting dykes are K-feldspar-rich (Figure 11-b). In weakly deformed parts mainly in the north-

east, orthopyroxene is preserved in the orthogneiss, indicating granulite facies conditions. This is mapped as such on the 1:100,000 scale map sheet (Grocott et al. 1987).
In the northeast, the orthogneiss is only weakly deformed and has a monzogranite composition (Rosa et al. 2016). Contact relationships between the monzogranitic orthogneiss and the migmatitic orthogneiss have not been observed and remain unclear.

Figure 11. *Svarthenhuk: a) Characteristic migmatite; b) Migmatitic orthogneiss with Kfs-rich dykes.*

Upernivik is characterised by grey, banded gneiss with amphibolite (hornblende-plagioclase-quartz-(biotite)) bands. The migmatitic banding in the gneiss is folded and transposed into shear zones with W-vergent deformation (Figure 12-a,b). The orthogneiss is frequently crosscut by pink pegmatite and microgranite dykes. On the west coast of Upernivik, granulite facies gneisses are preserved. Felsic migmatites consist of biotite-plagioclase-quartz-garnet with leucosomes containing plagioclase-quartz-hornblende-clinopyroxene-garnet (Figure 12-c). These rocks contain metre-scale mafic lenses, mapped as amphibolite (Figure 12-d). These lenses have clinopyroxene and orthopyroxene-rich centers, where clinopyroxene is locally rimmed by hornblende in contact with plagioclase. Leucosomes consist of orthopyroxene-plagioclase-quartz-(chalcopyrite) assemblages. Further west at Kigarsima, the rocks are similar, although not as well-exposed as on Upernivik. Felsic migmatite is composed of quartz-plagioclase-K-feldspar-hornblende-biotite and mafic lenses have leucosomes consisting of plagioclase-quartz-clinopyroxene-orthopyroxene.

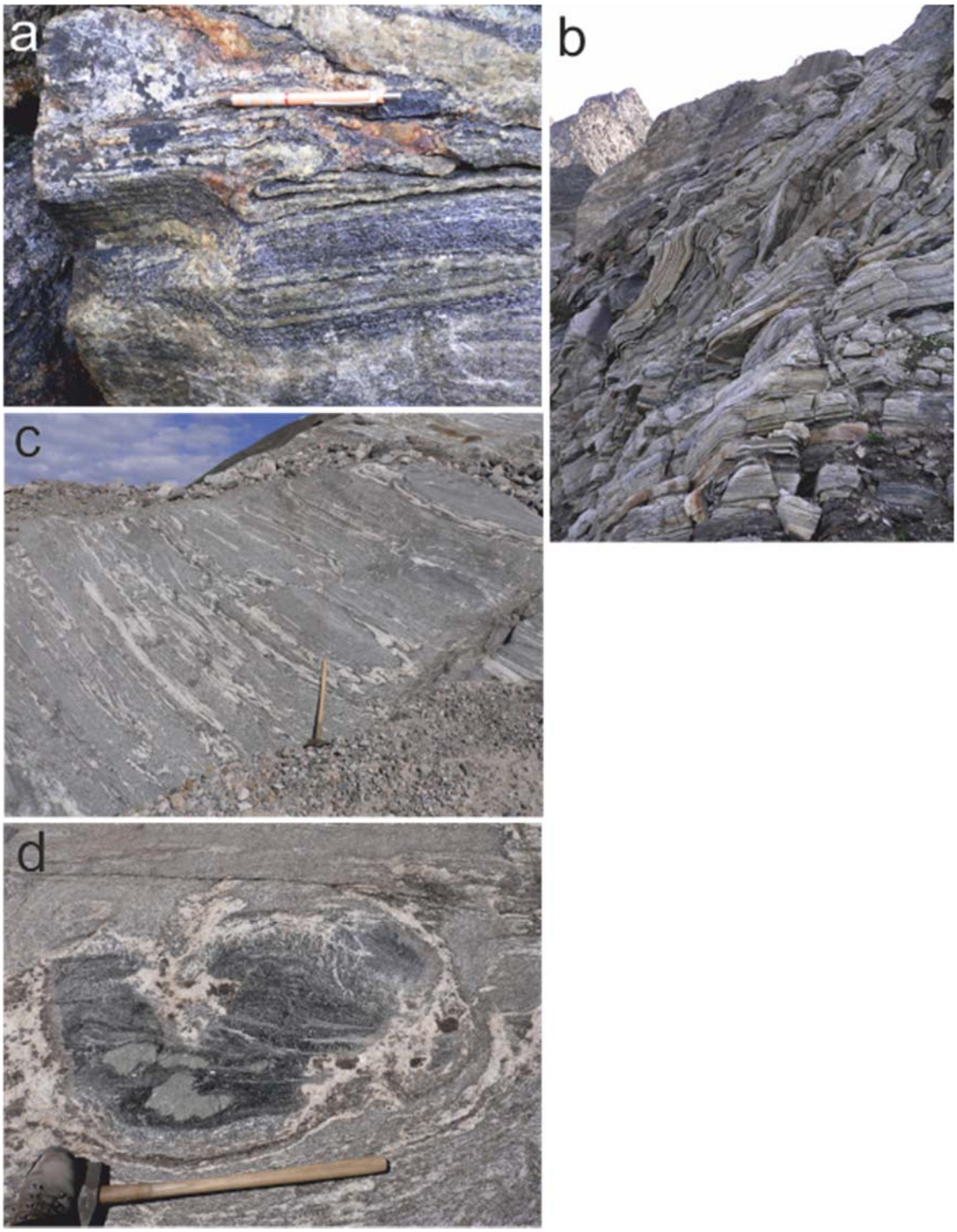

Figure 12. *Upernivik: a) Migmatite with isoclinally folded banding; b) Migmatite with amphibolite boudins transposed into a shear zone; c) Felsic migmatite from the west coast of Upernivik; d) Characteristically zoned mafic lens with leucosomes.*

At Kangerlussup Sermerssua, the Archean rocks are banded amphibolite with hornblende-garnet-plagioclase-quartz and clinopyroxene-hornblende-plagioclase-quartz bands. In the central parts of the amphibolite, orthopyroxene-clinopyroxene-plagioclase leucosomes are observed. The orthogneiss has a chloritic foliation at the top contact with Paleoproterozoic siliceous biotite gneiss. Lenses of ultramafic rocks (actinolite-chlorite-tremolite) also occur

along the contact. Also on the nunataks, migmatitic orthogneiss and mafic enclaves or lenses with clinopyroxene-plagioclase-orthopyroxene leucosomes characterise Archean rocks (Figure 13). Augengneiss forms rafts in the migmatite. This changes, interestingly, at RTZ Discovery (Coppard et al. 1992) and at a nunatak in central Alfred Wegener Halvø, where the orthogneiss is only foliated at lithological contacts and the overall appearance is that of a tonalite with hornblende-quartz-plagioclase-biotite. The felsic rocks have abundant xenoliths of biotite schist, black schist, paragneiss and plagioclase-quartz-biotite gneiss, and it should be ascertained whether they are Archean.

Figure 13. *Typical Archean migmatite of the Kangerlussup Sermerssua nunataks.*

Generally, three kinds of orthogneiss are distinguished around Maarmorilik: (1) medium-grained grey, locally porphyroclastic, orthogneiss, (2) coarse-grained light grey, locally porphyroclastic, orthogneiss, and (3) polyphase orthogneiss and migmatite. The coarse-grained light grey orthogneiss, locally with K-feldspar-augen, shows weakly tectonically reactivated intrusive contacts with the medium-grained grey orthogneiss (Figure 14-a). Both have a similar mineralogy of biotite-quartz-plagioclase-(hornblende-muscovite) and are cut by white plagioclase-quartz veins. A SE-vergent, normal greenschist facies shear zone separates these orthogneisses from the third type, which is a polyphase gneiss with in situ partial melting and melt-present deformation structures restricted to the leucosomes (Figure 14-b). A crumbly schist, indicating shearing at low metamorphic conditions, represents the contact with rocks of the Mârmorilik Formation (Figure 14-c).

Figure 14. *Maarmorilik: a) Grey porphyroclastic orthogneiss with ductile shear zone localised in whitish coarser grained part; b) Polyphase orthogneiss with agmatite structure; c) Crumbly schist at contact with overlying Paleoproterozoic meta-sedimentary rocks.*

On the western part of the Alfred Wegener peninsula, orthogneiss and amphibolite occur (Figure 15-a). A SE-vergent normal shear zone is developed, showing structures of melt-present deformation. A biotite-rich biotite-quartz-plagioclase gneiss with abundant leuco-somes represents a possible paragneiss and is mapped as augengneiss in the 1:100,000 scale map (Figure 15-b).

Figure 15. *Alfred Wegener peninsula: a) Deformed orthogneiss and amphibolite from the western part of the Alfred Wegener peninsula: b) Biotite-rich biotite-quartz-plagioclase gneiss that is mapped as augengneiss.*

Nunataq Formation

The Nunataq Formation consists of a complex sequence of amphibolite, quartzite, marble, chert, epidosite and meta-pelite to meta-psammite units that are exposed in a fold-like structure cored by Archean monzogranite gneiss. The contacts between the different units are always tectonic, and the rocks have a well-developed subvertical foliation that is locally mylonitic. In contrast to the volcano-sedimentary units of the Karrat Group, the Nunataq Formation records widespread evidence for hydrothermal alteration, with metamorphic grades ranging from peak amphibolite facies to retrograde greenschist facies conditions. The amphibolite layers have a mineral assemblage of hornblende, plagioclase, quartz ± clinopyroxene and are locally silicified. They are crosscut by abundant quartz-pyrite veins with hydrothermal actinolite-biotite-pyrite alteration (Figure 16-a). The veins locally show evidence of open space growth. Chlorite, epidote and titanite are possible hydrothermal alteration minerals as well. Shearing and hydrothermal alteration are retrograde in the greenschist facies. The amphibolite is locally intercalated with a fine-grained, striped rock that likely represents a felsic unit intercalated with amphibolite (Figure 16-b). The rock mainly consists of plagioclase, actinolite, quartz and chlorite, with minor amounts of epidote and titanite. Plagioclase is extensively replaced by sericite. Where present, quartzite is pyrite-bearing. Meta-pelitic units are made up of quartz, biotite, plagioclase and muscovite, and are similar to the meta-sedimentary rocks at the base of the Nûkavsak Formation. Locally, coarse-grained, biotite-rich mica schist with up to several cm large garnet porphyroblasts have been recorded. Epidosites reach a thickness of up to several metrs, and locally are brecciated in the surrounding amphibolites.

A short (~500 m) traverse from north to south through the Nunataq Formation amphibolite was done mainly for geochemical sampling in order to compare it to known Kangilleq Formation meta-volcanic rocks. The northern contact between the Nunataq Formation amphibolite and Archean orthogneiss is sheared and marked by ~50 cm of chlorite schist. The Nunataq Formation in this area consists of banded, fine-grained hornblende-plagioclase-rich amphibolite units (<1 – 20 m) alternating with ‘rusty’, very fine-grained, quartz-muscovite-biotite+/-feldspar-rich schist (<1 – 10 m). Contacts between the amphibolite and schist layers are sharp (Figure 16-c). Only locally does a finely laminated, chlorite-actinolite

schist occur that may have primary bedding preserved, and therefore may represent a mafic tuff unit.

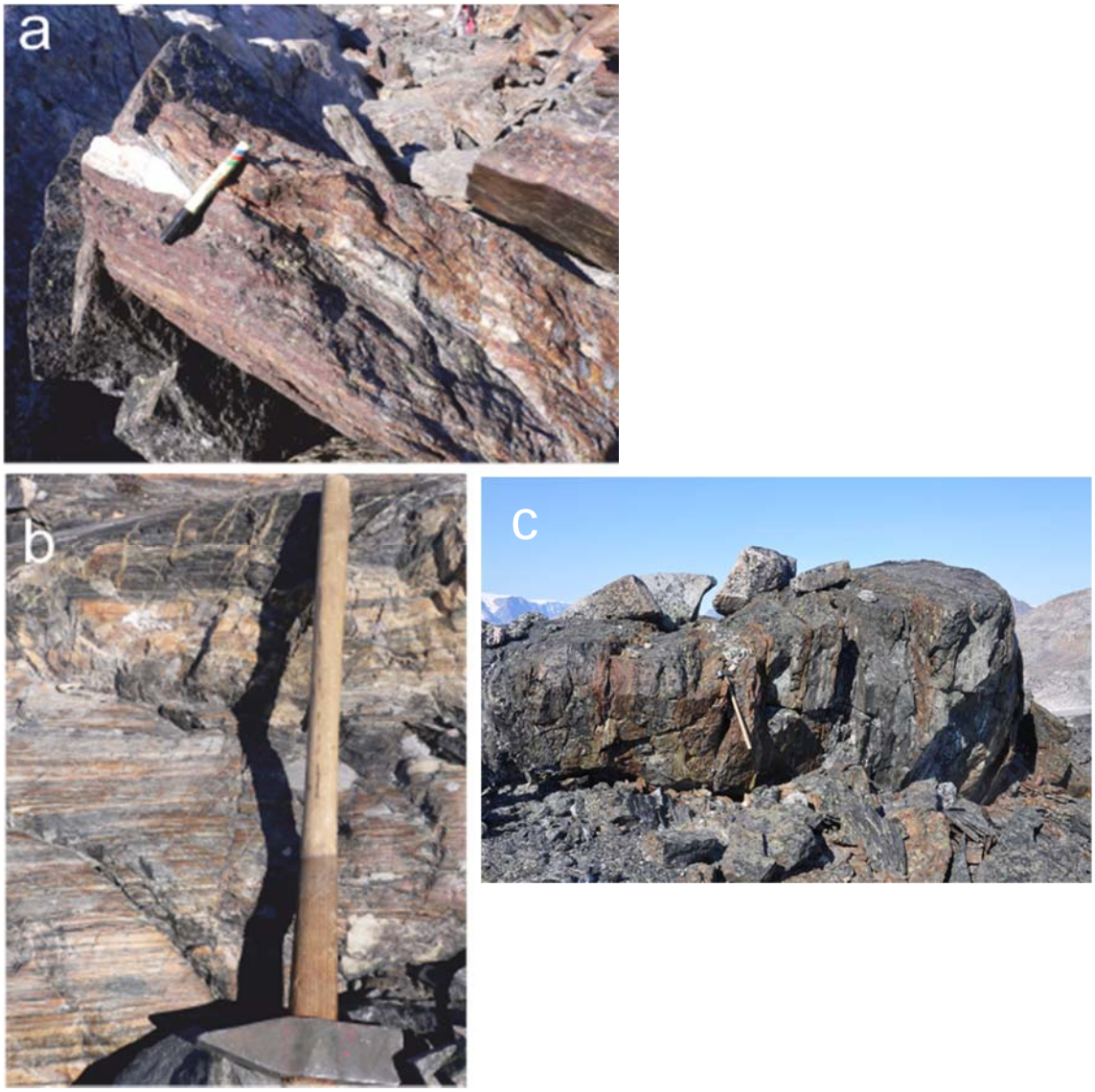

Figure 16. *Nunataq Formation: a) Quartz-pyrite veins in amphibolite with hydrothermal actinolite-biotite-pyrite alteration; b) Felsic (meta-volcanic?) rock consisting of plagioclase-quartz-chlorite-actinolite; c) Fine grained hornblende-plagioclase-rich amphibolite units alternating with 'rusty', very fine grained, quartz-muscovite-biotite+/-feldspar-rich schist layers.*

Stratigraphy of the Karrat Group

The Paleoproterozoic Karrat Group is a siliciclastic-carbonate-volcanic succession that was deposited unconformably on Archean crystalline basement rocks assigned to the Rae Craton. The Prøven Igneous Complex, which extends over a large area (about 100 km of coastline), divides supracrustal rocks of the Karrat Group into northern and southern exposures. The large spatial extent of the Karrat Group is a challenge for reconstructing stratigraphy and the architecture of the original sedimentary basin(s) and uncertainties remain as to the correlation of units across the region as well as its relationship to broadly coeval meta-sedimentary successions in the eastern Canadian arctic.

Three summers of reconnaissance mapping and detailed traverses have changed the original definition of the Karrat Group (cf. Henderson and Pulvertaft, 1967). These changes include the description of a new formation—the Qaarsukassak Formation (Guarnieri et al., 2016)— which hosts Zn-Pb mineralisation, as well as documentation of stratigraphic relationships between units, that has led to the division of an upper and lower Karrat Group. The Qeqertarssuaq Formation comprises the lower Karrat Group, whereas the Mârmorilik, Qaarsukassak, Kangilleq, and Nûkavsak formations comprise the upper Karrat Group. The Qeqertarssuaq Formation was never dated by Henderson and Pulvertaft (1967; 1987), but was assumed to be of Paleoproterozoic age. Moreover, the amphibolites and micaschists of the Qeqertarssuaq Formation indicate amphibolite facies conditions while the stratigraphically overlying Nûkavsak Formation typically records greenschist facies mineral assemblages, highlighting a break in the metamorphism across the contact. In the RTZ Discovery area, the Qaarsukassak Formation sits with angular unconformity on top of quartzites and garnet-amphibolites of the Qeqertarssuaq Formation (Guarnieri et al. 2016). Preliminary geochronological data for the Qaarsukassak Formation suggests that it was deposited in the Paleoproterozoic. Differences in depositional age and metamorphic grade suggest that the Qeqertarssuaq Formation might be unrelated to the remaining stratigraphy of the Karrat Group, or in the least, represents an angular unconformity.

Stratigraphy of the Karrat Group was investigated to understand the character, thickness, depositional environment, and relative conformity and correlation of the various units of the Karrat Group. Primary sedimentary or volcanic structures are preserved in most units of the upper Karrat Group, whereas they are not preserved in the lower Karrat Group. Well-defined stratigraphy leads to a better understanding of the basin tectonic setting(s) in which the Karrat Group was deposited and provides insights into how mineral potential relates to different stratigraphic units in space and time. The following is organised by stratigraphic unit within the Karrat Group, from oldest to youngest.

Undifferentiated Karrat Group

Supracrustal rocks at the head of Ukkusissat Fjord include a unit that is distinctly different from other Karrat Group units seen elsewhere. This quartz-feldspar ± garnet gneiss could not be confidently assigned to any unit of the Karrat Group (Figure 17). The paragneiss and garnet-paragneiss are intruded by a garnet-bearing granite ("white granite"). Pending zircon U-Pb geochronology on this unit will determine its age and relationship to units of the Karrat Group.

Figure 17. *Examples of the paragneiss in northern Ukkusissat Fjord.*

Qeqertarssuaq Formation

The lower Karrat Group is comprised of the Qeqertarssuaq Formation, which is best exposed in the region between the Kangilleq and Inngia fjord areas. The lower contact of the Qeqertarssuaq Formation has a tectonic contact with Archean basement rocks, and is overlain by supracrustal rocks of the Kangilleq and Nûkavsak formations. Though the Qeqertarssuaq Formation contains several different lithologies, the formation is typically characterised by quartzite, garnet mica schist, and amphibolite rocks. The following is a description of some of the localities visited in 2017.

A locality in Kussinersuup Aaffaa was visited to investigate the Qeqertarssuaq Formation – basement contact about 100 m below 2015 localities of Qeqertarssuaq Formation quartzites. Although the basement-Qeqertarssuaq Formation contact was expected there, instead paragneiss (quartz-biotite-feldspar), biotite-chlorite schist, quartzitic mylonite, and massive quartzite was found (Figure 18). At ~500 m elevation, a shear zone occurs with mylonites and boudins of non-mylontonised rock units. In contrast to what was expected, no clear contact between Archean basement rocks and Qeqertarssuaq Formation was found. The

paragneiss was attributed to the Qeqertarssuaq Formation. At ~1200 m elevation, we observed massive to banded grey to greenish quartzites in tectonic contact with muscovite-quartz mica schist boudins and chlorite-biotite schist. The rusty color change seen in the hillslope above 1200 m is secondary and not due to a lithology change (brown-weathering quartzites were observed in outcrop). This is an example of the importance of field-checking lithologies and contact relationships to confirm mapping by air or oblique photos.

Figure 18. *Paragneiss of the Qeqertarssuaq Formation (left) at Kussinersuup Aaffaa; massive quartzite occurs boundinaged (metre-scale) in quartzitic mylonite (right).*

In Kangilleq Fjord, at the Qangatarssuaq locality, Qeqertarssuaq quartzites are white to beige to pink in color, recrystallised with mm- to cm-scale banding and are homoclinal (Figure 19). These quartzites sometimes contain thin (~15 cm) bands of chlorite-biotite-quartz schist. Unlike other localities (e.g., Kussinersuup Aaffaa), quartzites are not mylonitic here. Above the white quartzite unit is a grey quartzite (trace muscovite, chlorite) with bands of mm-size magnetite grains concentrated in some layers. Outcrop is very limited near the cliff edge to Kangilleq fjord, and, though mapped as such, the contact with the ‘sp’ unit was not found here. About two kilometres to the north, outcrops of Qeqertarssuaq Formation occur out of stratigraphic order, i.e., tectonically above Kangilleq Formation rocks at the Qangatarssuaq locality. Though these Qeqertarssuaq Formation rocks are mapped as the ‘sp’ unit, the cliff was dominantly white and grey quartzites as seen below. The quartzites are folded (Figure 19), sometimes mylonitic, and contain some isolated boudins of calcite-quartz. The quartzite unit is overlain by grey phyllites near the top of the hill, which is in fault contact with actinolite-carbonate-quartz rocks of the Kangilleq Formation.

Figure 19. *White Qeqertarssuaq quartzite above the Qangatarssuaq locality in Kangilleq Fjord (left); folded Qeqertarssuaq quartzite that is tectonically-repeated, therefore occurring structurally above Kangilleq Formation rocks at the Qangatarssuaq locality (right).*

Quartzite and paragneiss outcrops, of uncertain age but which can possibly be assigned to the Qeqertarssuaq Formation, were identified in Pannertooq, Upernivik Ø, and Kigarsima.

Mârmorilik Formation

The Mârmorilik Formation is important since it hosts a world-class Zn-Pb deposit. Whereas the Mârmorilik Formation is overall dominated by carbonate rocks (dolomite to calcite marbles), the basal Mârmorilik Formation is dominated by siliclastic rocks, including quartzite, pebble to cobble conglomerate, and calcareous meta-sandstone. New localities visited in 2017 are described below.

Dolomite marbles are well exposed northeast of the 750 lake on the southeastern edge of the Maarmorilik area. Minor pyrite was observed along foliation planes in one area. Columnar stromatolites (Figure Figure 20) are preserved in grey finely-crystalline dolomite marble. Above these marbles is an interbedded succession of grey finely-laminated medium-grained non-calcareous meta-sandstone. The thickest sandstone layer is ~3m thick with a transitional contact to dolomite marbles, and intercalations on the scale of 10s of centimetres with orange-coloured dolomite marble on top (Figure 21).

Figure 20. *Rare stromatolites preserved in dolomite marble of the Mârmorilik Formation at the 750 Lake. Though Paleoproterozoic stromatolites are relatively common, they have not previously been documented in Mârmorilik Formation outcrops.*

Figure 21. *Sandstone-dolomite layers of the Mârmorilik Formation above observed stromatolite horizon.*

Though preserved as a sedimentary contact elsewhere in the Marmorilik area (Rosa et al., 2016), basal Mârmorilik Formation quartzites show evidence of minor shearing with Archean augengneissic basement rocks (Figure 22) on the Nunngarut Peninsula. The base of the Mârmorilik Formation at Nunngarut west is in contact with the Archean augengneiss. The contact with brown quartzites does not show evidence of shearing, suggesting a depositional contact. Several metres above the contact; however, a ~10 m thick mylonite zone occurs in Mârmorilik quartzite beneath dolomite-tremolite marble. About 8 metres of section are exposed below the mylonite down to the basement contact, comprised mainly of light brown quartzites and calc-silicate (calcite-quartz-tremolite) rocks (Figure 23). Dolomite marbles are exposed for several tens of metres above the mylonite, and are interbedded with a grey non-calcareous fine-grained meta-sandstone. Though folded, the meta-sandstone contains remnant scour structures and laminations. Though outcrop is sparse in this area, stream beds provide good exposures of grey laminated calcite marbles between two horizons of beige dolomite marble (Figure 24).

Figure 22. *Augengneiss (basement rocks) in contact with basal quartzite of the Mârmorilik Formation (also, right), showing minor shear.*

Figure 23. *Basal quartzite of the Mârmorilik Formation at Nunngarut west (left); mylonite within the lower Mârmorilik Formation at Nunngarut west (right).*

Figure 24. *Intercalated impure calcite marble and fine-grained meta-sandstone of the Mârmorilik Formation at Nunngarut west (left); dark grey laminated dolomite marble of the Mârmorilik Formation at Nunngarut west, stratigraphically above other photos (right).*

Qaarsukassak Formation

Similar to the Mârmorilik Formation, the Qaarsukassak Formation is of interest since it controls the distribution of Zn-Pb mineralisation, namely that identified by Coppard et al. (1992). The overall stratigraphy of the two formations, however, is quite different. The Qaarsukasak Formation is thin (2 to <50 m) compared to the Mârmorilik Formation (<2 km). The Qaarsukasak Formation is characterised by basal siliciclastic rocks, followed by thin calcite marble, and shale. Though previously thought to be spatially restricted to Kangerluarsuk Fjord (Guarnieri et al., 2016), a new exposure was discovered in 2017 in Umiamakku Isbræ, as described below.

Qaarsukassak stratigraphy at Kussinersuaq, in Umiammakku Isbræ (Figure 25) is similar to that of Kangerluarsuk Fjord, with about 30 metres of siliciclastic rocks (quartzite-psammite), followed by calcite marble, and shale (Figure 26). The quartzite-psammite unit at the base shows rare remnant cross-bedding, supporting right way-up younging direction. Orthogneiss basement rocks occur below the Qaarsukassak Formation, though the contact is covered. The rocks show some alteration (silicification, veining, sulfide mineralisation) and might be prospective for base metal mineralisation (see Economic Geology section).

Figure 25. *Oblique view of a new discovery of Qaarsukassak Formation (arrow points to rusty band at top of scree slope) at Kussinersuaq in Umiammakku Isbræ.*

Figure 26. *Qaarsukassak Formation at Kussinersuaq in Umiammakku Isbræ: Remnant cross-bedding in lower psammite-quartzite unit (top left), bedding in psammite-quartzite unit (top right), calcite marble (bottom left), shale in upper Qaarsukassak Formation (bottom right).*

At Qingaarssuaq, in Kangerlussuaq Fjord, a small section of Qaarsukasak-like meta-sedimentary rocks occurs above garnet-amphibolite and orthogneiss basement rocks. This thin (<3m) section of probable Qaarsukassak Formation consists of ~1.5 m of quartzite and psammite, ~40 cm calcite marble, and graphite schist (Figure 27). The Nûkavsak Formation occurs directly above the Qaarsukassak package.

Figure 27. *Section of Qaarsukassak Formation-like rocks at Qingaaarssuaq in Kangerlussuaq Fjord.*

Another minor section of Qaarsukassak Formation that was observed at Tornit, in Kangerluarsuk Fjord, is ~5 m thick (~3 m of impure calcite marble, ~2 m of fine-grained meta-sandstone/siltstone, overlain by ~60 cm of grey laminated calcite marble). A similar section was observed across the fjord, in Kigarsima.

A sedimentary contact is preserved between the Qaarsukassak Formation and basement rocks to the north of Qaarsukassak ridge in Kangerluarsuk Fjord. The basal unit is a ~2 m thick coarse to very coarse massive quartzite, which is overlain by a thin veneer (several cm) of conglomerate (Figure 28). The conglomerate contains subrounded to subangular clasts of predominantly quartzite pebbles (1 to 3 cm) and older meta-sedimentary rocks (fine-grained sandstone or psammite) in a sandy matrix. The quartzite-conglomerate is overlain by a fine to very fine grained sandstone (~1 m thick), overlain by a recrystallised dirty calcite marble (~1m). The upper contact with the Nûkavsak Formation is tectonic (sheared), indicated by a mylonite at the base of the Nûkavsak Formation (Figure 29, showing top to the ESE movement). A chlorite schist also occurs in the transition between the Qaarsukassak and Nûkavsak formations, which becomes a talc-siderite schist and is thrust repeated several times (ENE trending brittle thrust) in the lowermost part of the Nûkavsak Formation.

Figure 28. *Quartz-pebble conglomerate of the basal Qaarsukassak Formation to the north of Qaarsukassak ridge in Kangerluarsuk Fjord.*

Figure 29. *Mylonite at the base of the Nûkavsak Formation above the "paleovalley" section to the north of Qaarsukassak ridge in Kangerluarsuk Fjord.*

At Kangerluarsuup Sermia East, grey laminated to massive meta-sandstone of the Nûkavsak Formation occurs structurally below a section of calcite marbles, fine-grained sandstone, and pelite of the Qaarsukassak Formation. This area shows structural repetition of calcite marble-pelite-metasandstone (Figure 30) in east-verging thrusts, and drag folds that compromises thickness estimates, which falsely appear to be several hundreds of metres. Structurally-repeated sections such as Kangerluarsuup Sermia East represent possible mineralisation exploration targets.

Figure 30. *Section of Qaarsukassak Formation that structurally overlies the Nukavsak Formation at Kangerluarsuup Sermia East.*

At Kangerluarsuup Sermia West, the Qaarsukassak Formation is exposed on a nunatak that is dominantly composed of pyrite-graphite shale, calcite-tremolite marble, and fine-grained sandstone (Figure 31), which is similar to lithologies seen in Kangerluarsuup Sermia. Outcrop is extremely friable and difficult to access. Meta-sandstone of the Nûkavsak Formation are thrust on top of friable Qaarsukassak Formation rocks, as evidenced by a ~1.5 m mylonite at the base of the Nukavsak Formation. Only a few metres of Nûkavsak Formation are exposed here; the rest of the cliff below is structurally repeated Qaarsukassak Formation rocks (possibly up to 100 m).

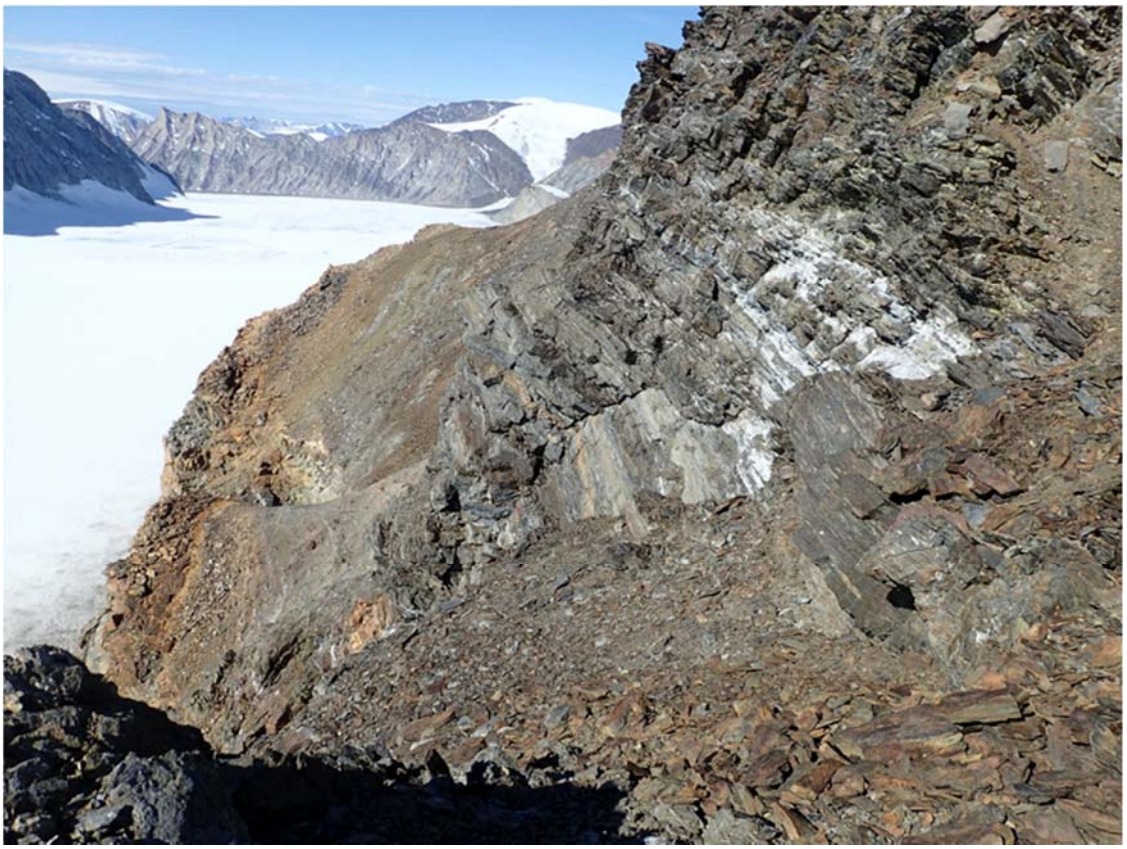

Figure 31. *Section of Qaarsukassak (bottom) and Nûkavsak (top) formations at Kangerluarsuup Sermia West nunatak.*

Kangilleq Formation

The Kangilleq Formation comprises the meta-volcanic rocks of the Karrat Group (Rosa et al. 2016, 2017). They are predominantly meta-basalts, metamorphosed to greenschist facies and dominated by chlorite with variable proportions of amphibole, carbonate, quartz, feldspar, titanite, rutile, Fe-oxides +- biotite (Rosa et al. 2016, 2017). Rocks of the Kangilleq Formation overlie the Qeqertarsuaq Formation or Archean orthogneissses, and are overlain by the Nûkavsak Formation, but also occur as discreet meta-volcanic packages within the Nûkavsak Formation. Primary volcanic textures include pillow lavas, pillow breccias, massive lavas, autoclastic breccias, and volcaniclastic rocks (tuff to breccias). The occurrence of pillow lava and hyaloclastite are unequivocal evidence of eruption in a subaqueous environment. Previous work defined the rocks of the Kangilleq Formation as alkaline (Rosa et al., 2016, 2017). However, preliminary whole rock trace element geochemistry (Zr/Ti and Nb/Y ratios) shows that rocks of the Kangilleq Formation plot as two distinct populations; subalkaline and alkaline basalts. Rocks of the Kangilleq Formation in the Kangilleq and Ingia fjords are alkaline basalt, whereas those of the Central Kangiusap Kuua are subalkaline basalt. At Southern Kangiusap Kuua, Nuugaatsiaq and Johannes Isbræ both signatures have been documented. The meta-volcanic rocks, that could possibly be Kangilleq Formation, found at Qiioqi/Inukassaat and Kangerlussup Sermerssua, display subalkaline signatures.

Meta-volcanic rocks of the Kangilleq Formation in the Central Kangiusap Kuua and at Nuugaatsiaq are dominated by mafic, scoria-rich breccias, characterised by sulfide mineralisation, and occur stratigraphically within the Nûkavsak Formation.

In the Central Kangiusap Kuua area the Kangilleq Formation is dominantly mafic in composition and comprises pillow lavas and tuff breccias (Rosa et al. 2017). The top of the volcanic sequence (~100 m true thickness) in this locality is marked by a rhyolite breccia that hosts stringer-type sulfide to massive sulfide mineralisation. The volcanic strata here is characterised by a subalkaline geochemical affinity.

Detailed mapping of volcanic lithofacies in the Nuugaatsiaq area suggests it is similar to volcanic stratigraphy as observed in the Central Kangiusap Kuua area. Meta-volcanic rocks at Nuugaatsiaq occur in two distinct northwest trending lenses and host Cu-Zn-sulfide mineralisation. The meta-volcanic rocks of the west lens are ~100 m thick and comprise a series of mafic tuff breccia and tuff units. The contact between the meta-volcanic rocks and the Nûkavsak Formation to the west is marked by an ~ 1 m wide ultramafic sill that cross cuts a mafic lapilli-tuff unit. Meta-volcanic rocks here are predominantly mafic breccias comprising scoria clasts (Figure 32). Normal grading and scour structures within these units indicate younging to the east. The contact with meta-sedimentary rocks of the overlying Nûkavsak Formation is not exposed; however, graded beds and cross beds indicate younging to the east, in agreement with the meta-volcanic rocks.

Figure 32. *Scoria-bearing mafic tuff breccia, Nuugaatsiaq area.*

Approximately 500 m of meta-sedimentary rocks of the Nûkavsak Formation separate the west and east lenses of meta-volcanic rocks. Graded beds within the Nûkavsak Formation indicate a change in younging to the west approximately 100 m west of the east lens. The

east meta-volcanic lens is ~20 m thick. To the west it is in sheared contact with graphite-silica-rich schist of the Nûkavsak Formation. The contact is sharp between the graphite schist and a 2-3 m thick, strongly carbonitised meta-volcaniclastic unit. Within this unit are lapilli- to block-size clasts of massive sulfide (Figure 33). This altered breccia is in sharp contact with relatively unaltered, mafic tuff breccia, mafic tuff and lapilli-tuff beds that are strongly foliated. A 2 m thick, strongly altered, coarse grained tremolite-ankerite-calcite-rich rock marks the contact with the Nûkavsak Formation to the east.

Figure 33. *Round, lapilli- to block-sized clasts of massive sulfide in a mafic tuff breccia (strongly carbonatised), Nuugaatsiaq area.*

Meta-volcanic rocks of the Kangilleq Formation in the Inngia and Kangilleq fjord areas are dominated by pillow lavas, with lesser massive lavas, and mafic volcaniclastic rocks. These basalts are geochemically different from those in the Central Kangiusap Kuua in that they are alkaline. Rocks of the Kangilleq Formation in this area overlie the Qeqertarssuaq Formation and are overlain by the Nûkavsak Formation. In contrast to the volcanic rocks at Central Kangiusap Kuua and Nuugaatsiaq there is no evidence of replacement of volcanic rocks with sulfide mineralisation.

The contact between greenschist facies meta-volcanic rocks of the Kangilleq Formation and amphibolite facies rocks of the underlying Qeqertarsuaq Formation has been described as unconformable (Rosa et al. 2016, 2017). Because this contact is locally sheared there remain questions about its nature.

Meta-volcanic rocks exposed in the Qangattarsuaq area on the north side of Kangilleq Fjord were mapped in detail during the 2016 field season. Samples from what was interpreted to be a silicified rhyolite and intermediate tuff of the Kangilleq Formation have preliminary U-Pb detrital zircon dates that are Archean. Consequently, the area was re-visited in 2017 to study the contact between the felsic rocks and the mafic meta-volcanic rocks of

the Kangilleq Formation in more detail. Upon further investigation, the contact between mafic meta-volcanic rocks of the Kangilleq Formation and the “silicified rhyolite” is sheared over <1 m, and marked by discontinuous quartz veins ranging from <1 to several metres thick. The wall rock is silicified (<2 m) below the quartz veins. The meta-volcanic rocks of the Kangilleq Formation, above the veins, are not silicified. The silicified zone is very fine grained with cm-scale gray and white banding. It is a sample of this silicified wall rock that yielded Archean zircons and as such is now interpreted to be silicified quartzite of the Qeqetarssuaq Formation. The intensely silificied unit is exposed over ~1.5 m before ending in overburden. Across ~ 20 m of overburden is a phyllite, inundated with quartz veins and weak to moderate, pervasive silicification. Along strike the phyllite becomes more schistose and contains both muscovite and staurolite.

These new observations suggest that in the Qangattarsuaq area there is a shear zone (1 – 5 m wide) between the mafic meta-volcanic rocks of the Kangilleq Formation, and quartzites and mica schists of the Qeqertarssuaq Formation, which is locally an ultramylonite. The ultramyonite was previously interpreted as an intermediate, plane-bedded tuff, and was the other sample from 2016 to yield Archean zircons. However, in the Qangattarsuaq area the contact between the Kangilleq Formation and underlying garnet-mica schists of the Qeqertarssuaq Formation is also observed to be undulatory yet sharp (i.e. no evidence of shearing). For this reason, and in order to document lithofacies and thickness changes, as well as any geochemical changes that may occur within the Kangilleq Formation, and to better understand the volcanic and tectonic environments in which it was erupted, three detailed stratigraphic sections were completed at: 1) Rinks Isbræ, 2) Puallarsiiviup Qooruua Valley Southeast, and 3) Umiammakku Isbræ.

A well exposed ~42 m thick section of Kangilleq Formation near Rinks Isbræ overlies strongly Fe-stained phyllite or slate. The lower contact is sheared with no primary/volcanic textures preserved in the lower 10 m of the Kangilleq Formation, which is a chlorite schist. Above this is ~25 m of 1-5 m thick, massive and pillowed basalt flows, with well-developed flow top breccias, commonly separated by planar laminated mafic tuff (<1 m; Figure 34). This is followed by ~ 10 m of basalt sheet flows with hyaloclastite that transition over 2 m into a pillowed flow (Figure 35). The pillows, which are strongly ankerite-silica altered are overlain by a massive, ~2 m thick ankerite-silica ‘cap’ rock that ends in overburden (Figures 36 and 37). The upper contact with the Nûkavsak Formation is not exposed.

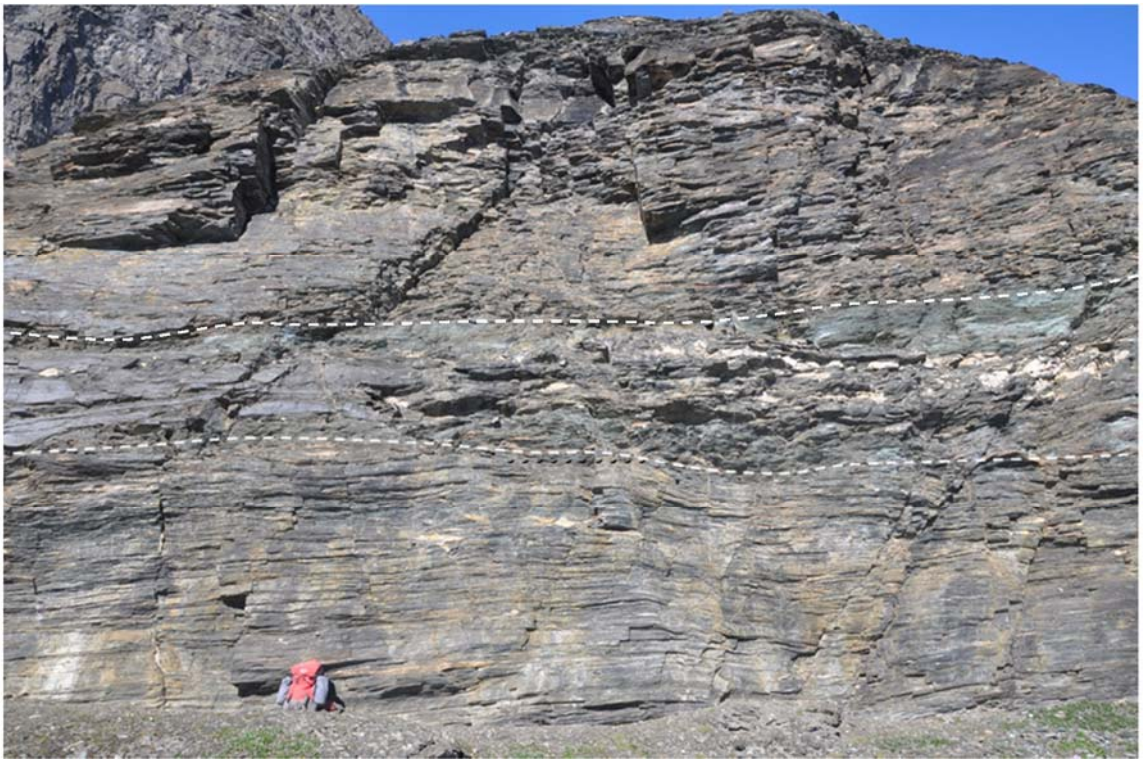

Figure 34. *From bottom to top: Banded basalt, mafic breccia to tuff (chlorite schist), pillow basalt.*

Figure 35. *Cross-section through pillow basalt.*

Figure 36. *Basalt sheet flows with hyaloclastite (left) overlain by pillow basalt that becomes progressively more carbonate and silica altered towards the top of the flow (right).*

Figure 37. *Very fine grained silica (+/- ankerite) 'cap' rock, Kangilleq Formation.*

Within the overlying Nûkavsak Formation, are two dark green units, each approximately 10 m thick (Figure 38). One is a fine grained actinolite-chlorite-silica-rich with a remnant clastic, and locally variolitic texture. The upper dark green unit contains clasts (lapilli- to block-size) that are aphyric, green, round and preferentially weathered. The unit also contains white, euhedral porphyroblasts of an unidentified mineral. Neither of the two dark green units within the Nûkavsak Formation resemble, mineralogically or texturally, the Kangilleq Formation volcanic rocks below.

Figure 38. *Mafic meta-volcanic units (thin dark horizontal bands above and below 'rusty' brown horizon near top of scree slope) with the Nûkavsak Formation, near Rinks Isbræ.*

An ~115 m section of the Kangilleq Formation near in the Umiammakku Isbræ is dominated by volcaniclastic rocks with lesser pillow and massive lavas. As in the Rinks Isbræ location the basal unit of the Kangilleq Formation in the Umiammakku Isbræ area is a chlorite schist. Discontinuous carbonate veining in the chlorite schist is common within several metres of the contact, which is sheared over ~60 cm and locally marked by a 30 cm-wide quartz vein. The underlying unit is a muscovite±staurolite schist. The dominant foliation in the schist (304/74) is different from that in the overlying basalt (287/35), which is parallel to the contact (Figure 39).

Figure 39. *Contact (dashed line) between banded mafic meta-volcanic rocks of the Kangilleq Formation (top) and muscovite schist of the Qeqertarssuaq Formation (bottom), Umiammakku Isbræ.*

Above the sheared lower contact the Kangilleq Formation is comprised of mafic tuff breccia beds (Figure 40), ranging in thickness from 10 – 50 m and characterised by block- and lapilli-size basalt clasts, with subordinate amounts of mafic lapilli tuff and tuff. The top of the Kangilleq Formation in this area comprises both massive and pillow basalt flows, ranging from 5 – 12 m in thickness, that transition upwards into flow top breccias (1 -2 m thick). The upper most unit of the Kangilleq Formation at this locality is a massive basalt flow and its upper contact is not exposed. Overlying the meta-volcanics rocks is a bedded, pale brown-grey, quartz-rich, meta-sedimentary rock that transitions over 1 m to a bedded, pale brown-orange (ankerite altered) rock with block-size scoria clasts (Figure 41). This unit gradually transitions over 20 m to grey meta-sandstones of the Nûkavsak Formation, with no ankerite alteration and no scoria clasts.

Figure 40. *Mafic tuff breccia. Round, vesicular basalt blocks in a very fine grained chloritised matrix, Umiammakku Isbræ area.*

Figure 41. *Possible scoria clasts in a very fine grained matrix of ankerite and silica, Umiammakku Isbræ area.*

An excellent exposure of an ~300 m section of the Kangilleq Formation southeast of Puallarsiiviup Qooruua Valley is dominated by pillow breccias with lesser pillows lavas. The base of the Kangilleq Formation is in sheared contact with an underlying mica schist of the Qeqertarssuaq Formation (Figure 42). As at Rinks Isbræ and Umiammakku Isbræ the lower contact between the meta-volcanics and underlying mica schist of the Qeqertarssuaq Formation is sheared. The basal unit of the Kangilleq Formation is a chlorite±biotite schist. The Kangilleq Formation in this area comprises planar laminated mafic tuff (~2 m), basalt sheet flows with interflow hyaloclastite (~ 10 m), a thick (~200 m) sequence of pillow breccias (50-85% block-sized, aphyric, vesicular pillow basalt fragments; Figure 43), and a sequence of pillow and massive lavas (~20 m) all capped by 2-4 m of interbedded fine grained siliceous rocks and coarse grained, strongly carbonatised, actinolite-rich rocks and 2-3 m of chert. The chert is overlain by meta-sandstones of the Nûkavsak Formation.

Figure 42. *Lower contact (dashed line) between Kangilleq Formation mafic volcanic rocks and underlying mica schist of the Qeqertarssuaq Formation, Puallarsiiviup Qooruua area.*

Figure 43. *Variably vesiculated pillow basalt fragments in a clast-supported tuff breccia unit, Kangilleq Formation, Puallarsiiviup Qooruua area.*

In the Pannertooq area an ~36 m thick (true thickness complicated by folds) meta-volcanic unit occurs. It has a sharp lower contact with an approximately 2 m thick quartzite (Figure 44) that is underlain by a garnet-mica-bearing gneissic rock. The upper contact of the meta-volcanic unit with meta-sandstones is marked by an ~50 cm wide pegmatite sill (Figure 45).

Figure 44. *Lower contact (dashed line) between meta-basalt of the Kangilleq Formation and underlying quartzite of the Qeqertarssuaq Formation (bottom), Pannertooq area.*

Figure 45. *Pegmatite (arrow) along upper contact between meta-basalt of the Kangilleq Formation and overlying meta-sandstone of the Nûkavsak Formation, Pannertooq area.*

The meta-volcanic rocks in this area are dark green to black, strongly foliated, and tightly folded. They are characterised by centimetre-scale banding that alternates between dark green-black amphibole-biotite-rich layers and light green-white, very fine grained calcite-epidote-quartz-rich layers. Locally there are beds with volcaniclastic textures preserved ranging from lapilli-tuff to tuff breccia (Figure 46).

Figure 46. *Calcite-epidote-rich clasts in an amphibole-biotite-rich matrix of a tuff breccia bed, Kangilleq Formation, Pannertooq area.*

The underlying quartzite and garnet-bearing gneiss are interpreted to be part of the Qeqertarssuaq Formation and the overlying biotite-muscovite schist part of the Nûkavsak Formation and, as such, the meta-volcanic rocks are interpreted as the Kangilleq Formation.

Several other localities, described below, of meta-volcanic rocks (amphibolites) were mapped and sampled in order to determine if they are part of the Kangilleq Formation. In each case primary volcanic textures are not preserved; therefore, these amphibolite units cannot, at this point, be correlated with other meta-volcanic rocks in the region. At each location samples were collected for whole rock major and trace element geochemical and petrographic analyses for further comparison to known Kangilleq Formation meta-volcanic rocks.

In the waterfall area, east of Anchorage #3, there is a previously mapped amphibole-rich unit. Preliminary observations from 2016 suggested it is meta-volcanic rock of the Kangilleq Formation. The lower contact is in sheared contact (~50 cm) with a silicified, Fe-stained, locally malachite stained, meta-sedimentary unit (quartzite?). The upper contact with grey meta-sandstone of the Nûkavsak Formation is sharp, but irregular. The unit is banded, alternating between dark green-light green bands (chlorite-actinolite-rich) and brown-black bands (biotite-rich), very fine grained, and strongly foliated (Figure 47). Locally the unit has weak, pervasive silicification, and contains augen-shaped quartz masses (<1 – 25 cm) and quartz+/-calcite veinlets. There is no evidence of volcanic textures preserved in this unit.

Figure 47. *Chlorite-actinolite schist. No primary textures are preserved.*

A previously mapped amphibolite in the Kangerluarsuup Sermia area was also investigated. The lower contact of the amphibolite is sharp, but irregular, with Archean basement gneiss. The amphibolite is ~10 m thick, black, fine to medium grained, banded, hornblende-plagioclase-rich rock (Figure 48). The upper contact with grey, meta-sandstone of the Nûkavsak Formation is sharp. Within the Nûkavsak, ~1 m from the lower contact, is a <1 m thick amphibolite band. Its contacts with the Nûkavsak are sharp.

Figure 48*. Fine grained, banded amphibolite.*

In the Qiioqi Peninsula the contact between the gneissic basement and the Karrat Group is exposed. Along the western coast of Qiioqi, as well as at Kangerlussup Sermerssua, the contact is defined by a zone of mafic bands that separates the underlying gneiss from the overlying Nûkavsak Formation interpreted to represent amphibolite. These amphibolite bands are in places heavily intruded by pegmatite veins and bodies up to several tens of metres across (Baker, 2017).

At the southern edge of the Kangerlussup Sermerssua glacier(Figure 1) the Karrat Group rocks consist of a few thin (1-3m thick) bands of fine- to medium-grained amphibolite interbedded with 0.5-1 m thick bands of meta-sediments (Figures 49 and 50). The supracrustal rocks and the amphibolite in particular are strongly sheared. The meta-sediments are biotite-quartz-rich schists with cm-bands reminiscent of graded bedding in fine- to medium grained meta-sandstone. Because there cannot be detected any abrupt change in the outcrops in the slopes above this locality, the meta-sediments are considered part of the Nûkavsak Formation. A similar contact relationship, although not as well exposed, is found in the NW of the Qiioqi Peninsula, at the Inukassaat sound. Here, gneisses with mylonite bands in the upper part of the exposures are overlain by ca. 50 m of amphibolite scree. The amphibolite is fine-grained and foliated and is in turn overlain by > 100 m thick meta-sediments consisting of mica-schists with sandy portions and several rusty, graphite-bearing Fe-sulphide beds that are 0.2-0.5 cm thick. As for the meta-sediments described at Kangerlup Sermersuua, this package of mica schists and meta-sandstones appears transitional into grey Nûkavsak Formation meta-sediments several hundred metres further up the slope and persists monotonously to the top of the mountain. The meta-sediments at this locality are therefore, because of their lithological characteristics, interpreted to represent the lower part of the Nûkavsak Formation. Similar contact relationships are observed 7 km to the south at 1100 m elevation above the Inukassaat Sound.

Figure 49. *Immediately above the contact to the gneissic basement rocks (in the scree), ~5m thick package of alternating amphibolite and meta-sediment at Kangerlusuup Sermersuua.*

Figure 50. *~0.5m thick band of meta-sediment sandwiched between amphibolite in Fig. 49. Note the ~1 cm thick band of amphibolite some 5 cm above the hammer head and the graded bed 3 cm below this amphibolite.*

Nûkavsak Formation

The Nûkavsak Formation, the youngest unit of the Karrat Group, is predominately sand-dominated siliciclastic facies. This thick unit (structural thickness up to 5 km; Grocott and Pulvertaft, 1990; actual stratigraphic thickness is unknown) occurs in depositional contact with the Kangilleq Formation. The Nûkavsak Formation overlies either the Qeqertarssuaq, Qaarsukassak, or Kangilleq formations, or directly overlies Archean crystalline rocks, complicating the reconstruction of the basin architecture. Described below are some new localities visited in 2017, including a description of stratigraphic relationships between the Nûkavsak Formation and meta-volcanic rocks assigned to the Kangilleq Formation.

Meta-volcanic rocks occur within the Nûkavsak Formation on Nuugaatsiaq peninsula, though it is unclear from previous mapping if these rocks are interbedded or tectonically interleaved. The Nûkavsak Formation appears to be in depositional contact with volcanic rocks here. Sedimentary structures (e.g., scour structures) determine the succession to be right way-up, younging to the ~ENE (Figure 51). The meta-volcanic rocks, are mafic volcaniclastic lithofacies, tuff and tuff breccia, largely comprised of scoria clasts, and interpreted to be possibly correlative with the subalkaline meta-volcanic rocks of the Kangilleq Formation (i.e. those in the Central Kangiusap Kuua). Additionally, a ~5 m thick package of siliciclastic rocks similar in character to Nûkavsak Formation occurs within the meta-volcanic package. The meta-volcanic rocks are overlain by turbiditic flows of the Nûkavsak Formation. A gabbro dyke (~20 cm wide) intrudes the Nûkavsak Formation. Sedimentary structures in the Nûkavsak Formation include graded bedding, scour structures, and cross-bedding. The younging direction changes from stratigraphic-up to the ENE to stratigraphic-up to the WSW, indicated by cross-bedding and graded bedding, respectively (Figure 51). The younging direction changes before the next lens of meta-volcanic rocks of the Kangilleq Formation. This succession shows structural repetition, supported by the reverse younging direction of the Nûkavsak Formation. The stratigraphic position within Nûkavsak Formation (rather than below it) suggests these volcanic rocks might possibly represent a younger phase of volcanism.

Figure 51. *Nûkavsak-Kangilleq(?) formations on Nuugaatsiaq peninsula. Scour structure in Nûkavsak Formation indicating right way-up younging direction (top left); graded bedding in Nûkavsak Formation (top right); cross-bedding in Nûkavsak Formation (bottom left); volcanic breccia within Nûkavsak Formation.*

Owing to exposure obscured by heavy lichen-cover and moss, outcrops of Nûkavsak Formation at southern Kangiusap Kuua are somewhat unremarkable. Bedding is subvertical and without confirmation of way-up indicators from sedimentary structures, it is unclear if the section is overturned. Outcrops of Nûkavsak Formation show little variation in this area, from fine to coarse grained, ~10% biotite and typically massive, with rare remnant graded bedding (Figure 52). Ankerite occurs in cleavage planes of rusty-colored fine-grained metasandstone. A graphitic schist with well-developed crenulation cleavage becomes a common rock type, often with rusty lenses (no visible sulfides). Walking towards the river valley, volcaniclastic rocks and actinolite-bearing tuff(?) with lenses of amphibolite are overlain by a quartz-biotite schist. The volcaniclastic rocks might be sourced from mafic lavas to the north in Kangiusap Kuua.

Figure 52. *Example of Nûkavsak Formation with remnant graded bedding at southern Kangiusap Kuua.*

A reconnaissance traverse in northern Kangiusap Kuua confirmed that the molybdenite is associated with a green, propylitically-altered intrusion and not with quartz veins or a younger intrusion. Country rocks intruded are a rusty, quartz-rich lithology (silicified rhyolite? quartzite?) and volcaniclastic rocks (have biotite-quartz clasts and possible rhyolite clasts), which might belong to the Qeqertarssuaq and/or Kangilleq formations (Figure 53). It does not intrude the Nûkavsak Formation. Samples of the intrusion and country rocks were collected for petrography and whole rock geochemistry to understand the original composition of the intrusion. The intrusion-country rock panel might be a klippe within Nûkavsak Formation (as in central Kangiusap Kuua). A tonalite cross-cuts all units at this locality, implying that the intrusion post-dates thrusting.

Figure 53. *Green, propylitically-altered intrusion in northern Kangiusap Kuua (left), the same intrusion cross-cutting rusty quartz-rich country rocks (right).*

The dominant geological unit within Ukkusissat fjord was confirmed to be Nûkavsak Formation. Several stops were made by rubber boat sailing south in Ukkusissat fjord. Pegmatitic granites intrude the Nûkavsak Formation in several places (Figure 54) and some rocks of the Nûkavsak Formation contain massive tourmaline or garnet.

Figure 54. *Nûkavsak Formation in Ukkusissat fjord. Boudinaged pegmatitic granite in Nûkavsak Formation (left); less deformed Nûkavsak Formation near end of boat traverse (right).*

The Saattukujooq locality (Figure 55), at the northwestern margin of the Mârmorilik map sheet near the edge of the entrance to Kangilleq Fjord, was visited to investigate the previously mapped contact between basement rocks and Nûkavsak Formation. Unfortunately, no basement rocks are exposed at this locality. Either Qaarsukassak, or Kangilleq formation rocks were expected at this locality, according to oblique photos. Above a large talus slope, rusty-brown Nukavsak Formation is (structurally?) overlain by black rocks that look like meta-volcanic rocks of the Kangilleq Formation (Figure 56). Heterogeneous textures, including calcite alteration, and epidote-rich layers suggest volcaniclastic rocks, but no primary textures are preserved. A massive sulfide horizon is hosted in between meta-

sandstone and silicified chlorite-schist. Massive sulfide occurs as cabbage head morphology within a metre-size boudin. Meta-volcanic rocks are exposed for at least 4-5 metres and are in thrust contact with garnet mica schist. A second massive sulfide horizon was found along strike to the east, where it occurs at a thrust contact with garnet mica schist and a silicified chlorite schist (Figure 56). The garnet mica schist is infolded with the meta-volcanic rocks in this shear zone.

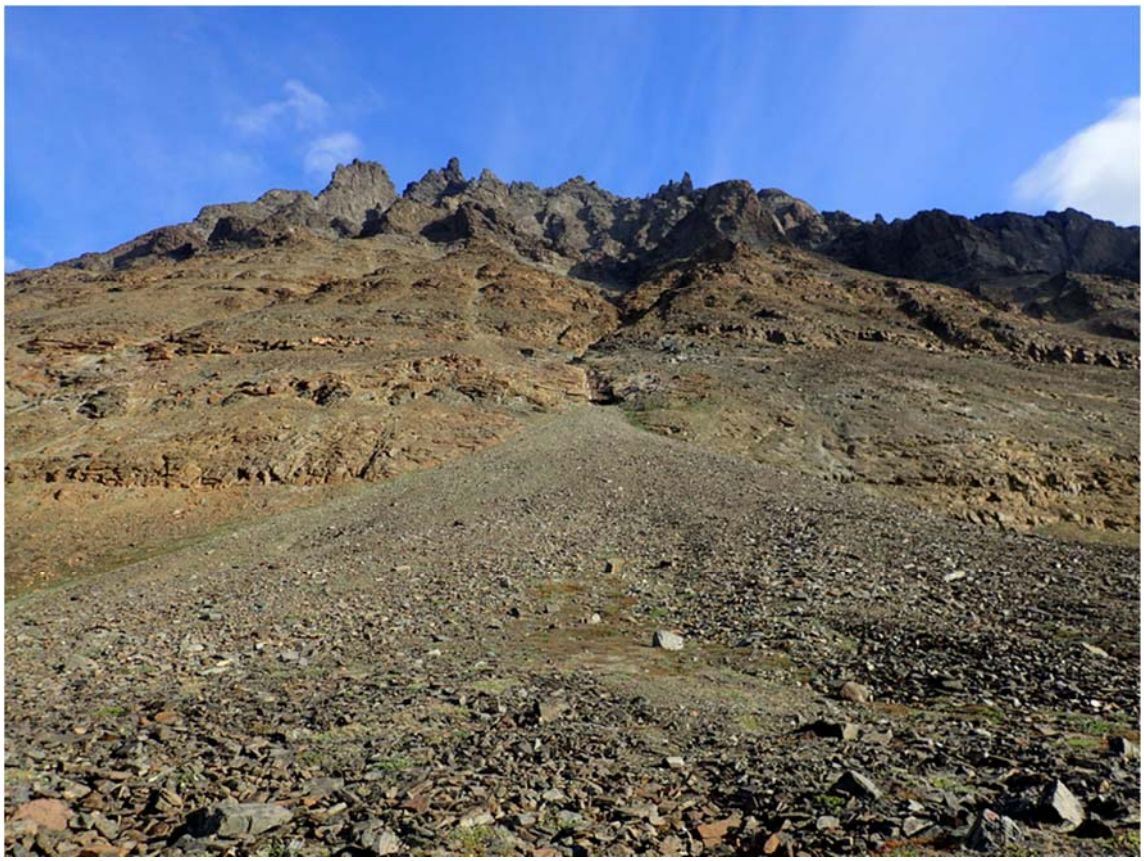

Figure 55. *Saattukujooq locality at the northwestern margin of the Mârmorilik map sheet.*

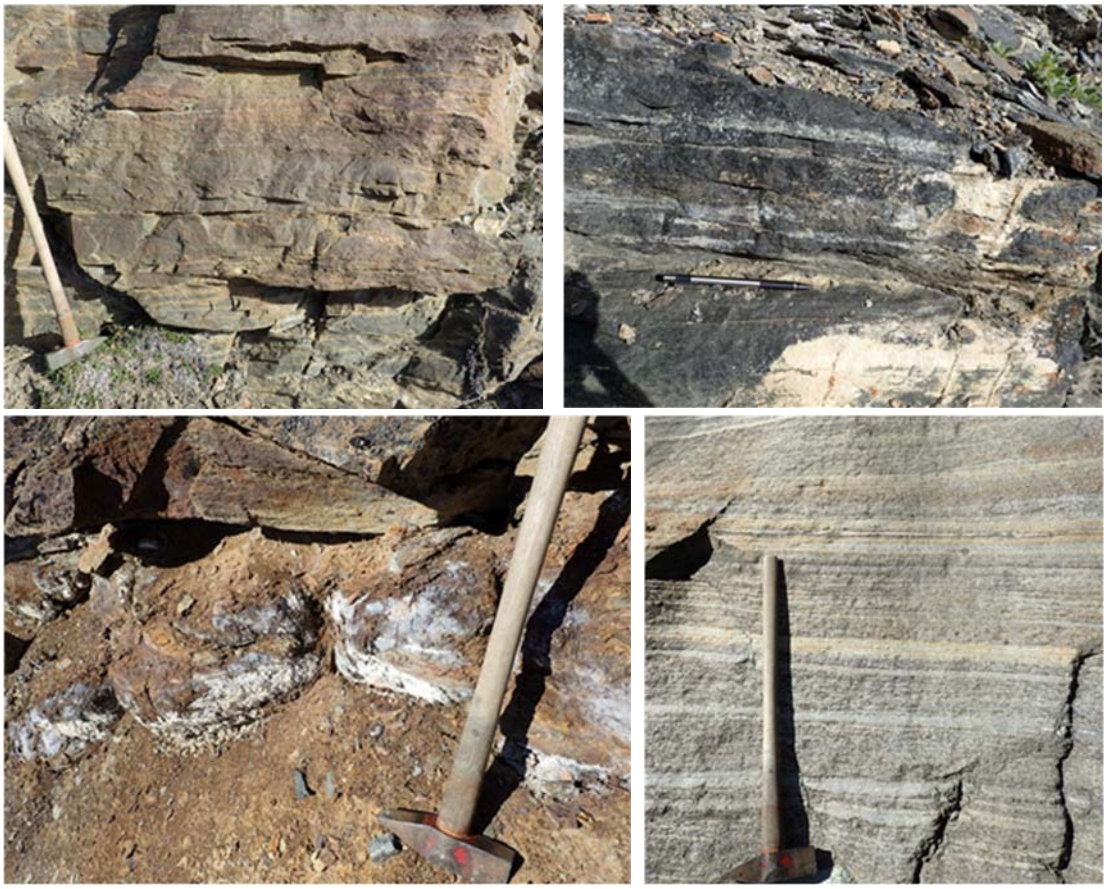

Figure 56. *Nûkavsak Formation (top left); Kangilleq (?) rocks (top right); massive sulfide horizon (bottom left); garnet-mica gneiss (Qeqertarssuaq Formation; bottom right).*

The Nûkavsak Formation in Kangerluarsuk Fjord (south of the RTZ Discovery area) is poorly exposed and heavily lichen covered. Where it could be observed, it is dominantly a medium-grained meta-sandstone with little lithological variation (Figure 57). No sedimentary structures were observed. Shear zones were present, best indicated by asymmetric quartz veins, indicating top to the east movement. Also notable was a graphitic pelite upsection, which was approximately 3 m in thickness (Figure 58).

Figure 57. *Though dominantly lichen-covered in this area, this outcrop of Nûkavsak Formation is a medium-grained meta-sandstone.*

Figure 58. *Thin (~3m) graphitic pelite in otherwise monotonous medium-grained meta-sandstone of the Nûkavsak Formation.*

Summary

New localities of Qaarsukassak Formation were discovered and described in 2017, including: Kussinersuaq in Umiammakku Isbræ, Rinks Isbræ, Qingaarssuaq in Kangerlussuaq Fjord, Kigarsima/Tornit in Kangerluarsuk Fjord, and Kangerluarsuup Sermia. These sec-

tions show stratigraphic similarities to the Qaarsukassak Formation in its type section at the RTZ Discovery area (Coppard et al. 1992), in Kangerluarsuk Fjord. The Qaarsukassak Formation was also observed in another section north of Qaarsukassak ridge, in Kangerluarsuk Fjord (the “paleovalleys” previously described by Guarnieri et al., 2016).

Rocks of the Kangilleq Formation occur stratigraphically between the Qeqertarssuaq and Nûkavsak formations, but also occur as discrete meta-volcanic packages within the Nûkavsak Formation. The latter (Central Kangiusap Kuua) are subalkaline, while the former (Kangilleq and Inngia fjords) are alkaline. Thus, it appears that the rocks of the Kangilleq Formation can be subdivided, based on stratigraphic relationships and whole rock geochemistry, into two units.

Mafic volcaniclastic rocks in the Nuugaatsiaq area contain similar lithofacies (mafic tuff breccias dominated by scoria blocks) and massive sulfide mineralisation to those at Central Kangiusap Kuua (no massive sulfide is observed within alkaline volcanic rocks of the Kangilleq Formation).

New observations of the lower contact of the Kangilleq Formation in the Qangattarsuaq area show that locally greenschist facies meta-volcanic rocks the Kangilleq Formation are in sheared contact with a quartzite of the Qeqertarssuaq Formation, and locally they are in sharp, unconformable, but not sheared, contact with a garnet-mica schist of the Qeqertarssuaq Formation.

Comparison of stratigraphic sections through the Kangilleq Formation in the area of Puallarsiiviup Valley Southeast and Umiammakku Isbræ, indicate that the formation is dominated by mafic tuff breccias with subordinate pillow and massive basalt lavas. In contrast, the stratigraphy observed in the Qangattarsuaq area and Rinks Isbræ is dominated by alternating, pillow and massive basalt lava flows with lesser mafic volcaniclastic rocks. This suggests a dynamic seafloor environment for the emplacement of the Kangilleq Formation, likely one in which synvolcanic faulting caused the formation of one or more basins restricting both the deposition of volcaniclastic debris, and the distribution of lava flows.

There is no evidence of pyroclastic eruptions, no evidence of emergence, and no bedforms indicative of a depositional environment that is above storm wave base within the Kangilleq Formation; therefore, the only restriction on water depth for deposition is >200 m.

Amphibolite units in the Pannertooq area locally preserve volcaniclastic textures (lapilli- and block-size volcanic clasts). This combined with their stratigraphic position between the Qeqertarssuaq and Nûkavsak formations suggests they are Kangilleq Formation. Further petrographic and geochemical observations are required in order to better understand the petrogenesis of this unit, in particular to determine whether it has alkaline or sublkaline affinities.

Amphibolite units in the Kangerluarsuup Sermia, Kangerlussup Sermerssua and Qiioqi/Inukassaat areas are between Archean basement gneiss, or mica schists, and below

meta-sandstones of the Nûkavsak Formation. As such it is possible that these unit represent volcanic rocks of the Kangilleq Formation. Further petrographic and geochemical observations are required in order to better understand the petrogenesis of these amphibolite units and to compare them to meta-volcanic rocks of the Kangilleq Formation.

The presence of stromatolites was hypothesised in Mârmorilik dolomite marbles, but had not yet been discovered. Stromatolites were found in less deformed Mârmorilik Formation outcrops near the 750 Lake.

Relationship between PIC and Karrat Group

The Prøven Igneous Complex (PIC) is exposed between *c.*72˚15´N and 73˚10´N in the Rinkian Orogen of central West Greenland (Escher & Pulvertaft 1976). To the north and south of the complex the Rinkian Orogen has been mapped in detail (Escher & Stecher 1978, 1980; Escher & Pulvertaft 1968; Henderson & Pulvertaft 1967, 1987). However, the resultant series of published 1:100,000 map sheets do not cover the main part of the PIC or most of its northern and southern contacts, although the area is covered by 1:500,000 survey mapping and unpublished field maps of the PIC at 1:40,000-scale are held in GEUS archives. The PIC occupies an important place in the regional geology of the Rinkian Orogen and hence in the overall tectonic context for the setting of mineral deposits in the belt. In 2017, a special field study was initiated to clarify the relationship between emplacement of the PIC and deformation/metamorphic events as part of on-going work on the KarratZinc project and in the light of recent field observations and published geochronological results (Rosa et al. 2016, 2017; Sanborn-Barrie et al. 2017).

The main rock type in the PIC is hypersthene granite (charnockite) often with K-feldspar phenocrysts (Escher & Pulvertaft 1976). It has been dated by Thrane et al. (2005) who obtained a U-Pb SHRIMP age of 1869 ± 9 Ma for a marginal phase of the PIC. This age refined an Rb-Sr whole rock isochron age determined by Kalsbeek (1981). At the northern and southern margins of the PIC, geological survey mapping shows a close spatial relationship between charnockite and garnet leucogranite. Prior to the current study, it was known that both the northern and southern boundaries of the PIC dip inwards (Escher & Pulvertaft 1968; Grocott & Vissers, 1984). The tectonic nature of these boundaries, as well as the NW-NNW kinematics in the north and the E kinematics in the south, were established during the previous field season (Rosa et al., 2017). Below each contact of the hypersthene granite, sheets of garnet leucogranite were emplaced into already strongly foliated metasedimentary host rocks (Grocott & Pulvertaft 1990). The leucogranite sheets are often folded and boudinaged and strong deformation has erased most intrusive contacts but some sheets are discordant to strongly discordant and it appears that they were emplaced as syn- to post-tectonic intrusions in a high-temperature zone of intense ductile deformation. In view of the spatial relationship between the leucogranite and the PIC, a crucial assumption made by earlier researchers was that *both* the leucogranite and hypersthene granite were syn- to post-tectonic and that therefore the age of *c.*1869 Ma for the hypersthene granite was also the age of deformation and high-temperature metamorphism in the meta-sedimentary rocks *and* of the PIC (Grocott & Pulvertaft 1990). This interpretation has been questioned by Rosa et al (2016, 2017). Recent geochronological results show that a re-evaluation of this assumption is necessary with implications for the timing of PIC emplacement relative to regional structural development and for metamorphic history (Sanborn-Barrie et al. 2017).

New U-Pb ages for charnockite intrusions of the PIC; including a quartz diorite, a quartz monzonite and a granodiorite yield crystallisation ages of 1876 ± 4 Ma, 1893 ± 9 Ma and 1900 ± 4 Ma respectively (Sanborn-Barrie et al. 2017). This establishes an age-range for PIC emplacement of *c.*1.90-1.87 Ga; distinctly earlier than previous age determinations for the emplacement of the complex. In addition, new ages of zircon overgrowths on detrital

zircon cores in meta-sedimentary rocks do not support the idea that the regional high-temperature metamorphism and emplacement of leucogranite sheets necessarily took place at about the same time as the PIC was emplaced. In the Lower Karrat Group south and north of the PIC, un-zoned rims of detrital zircon grains yield ages of *c.*1822 and 1840 Ma, interpreted to represent an episode of metamorphism (Thrane, 2005; Sanborn-Barrie et al. 2017).

Atilissuaq (72˚47.830´N; 55˚53.750´W):
On the island of Atilissuaq three main lithological units; quartzite, migmatitic paragneiss, and charnockite are exposed (Figure 1). Quartzite is medium- to coarse-grained, and is characterised by a well-defined layering that is here interpreted as transposed bedding (Figure 59). In addition to quartz, the rock contains traces of fine-grained biotite, clinopyroxene, muscovite and amphibole. The migmatitic paragneiss is fine- to medium-grained and has a peak metamorphic mineral assemblage of orthopyroxene, biotite, plagioclase, ilmenite and quartz, and locally, garnet and/or cordierite, indicating granulite facies conditions (Figure 60). The rock is commonly rusty. The migmatitic paragneiss contains abundant leucosomes that vary in thickness between a few mm to several cm. The leucosomes contain garnet and commonly orthopyroxene, implying that they reflect peritectic phases formed during partial melting. The well-developed foliation is defined by the alignment of peak metamorphic minerals and most of the leucosomes. The charnockite of the PIC is a massive, typically greenish, medium- to coarse-grained and weakly to moderately foliated gneiss with a peak metamorphic mineral assemblage of garnet + orthopyroxene + K-feldspar + biotite + plagioclase + quartz + opaques. The volume of leucosomes is relatively low compared to the migmatitic paragneiss. In weakly deformed domains, both magmatic and crystal-plastic fabrics have been preserved, and the rock locally contains up to several cm-large feldspar phenocrysts. The contact between the PIC and the migmatitic paragneiss is always tectonic and parallel to the foliation in both types of rock.

Figure 59. *Compositional layering in quartzite at 72° 47' 37.4388" N; 55° 51' 53.6904" W.*

Figure 60. *Migmatitic paragneiss, showing a peak metamorphic mineral assemblage of garnet, orthopyroxene, plagioclase and quartz (72° 47' 38.9198" N; 55° 53' 12.7334" W).*

The boundaries between quartzite, paragneiss and the PIC appear parallel to the main planar fabric which, in the sedimentary lithologies, is defined by bedding transposed to differentiated layering and, in the PIC, by a crystal-plastic deformation fabric and flattened leucosome patches (Figure 61). At a district scale, published geological survey mapping implies that the paragneiss precursor sedimentary rocks overstepped to the SW from the rather thick sequence of quartzite exposed on Atilissuaq onto thinner quartzite, and even onto Archean basement on Lange Ø and Upernavik Ø (Figure 1). Contacts between all three major rock units and planar fabrics are folded by an upright fold: the Atilissuaq anticline (Figure 1). The fold trends NE-SW and has an elongated, dome-like shape. In the hinge, a weak planar fabric parallel to the axial surface intersects the main fabric to form a S- to SW-plunging intersection lineation. This lineation is probably parallel to the plunge of the large-scale fold. The main unit of the PIC on the Atilissuaq island is a ~1.5km-thick charnockite sheet with large K-feldspar phenocrysts. Exposures are often weathered to a copper-colour with well-spaced joint systems. This unit is exposed also on the adjacent island of Qaarsorsuaq (Figure 62).

Figure 61. *Leucosome patches in PIC flattened to lie parallel with crystal-plastic fabric defined by hypersthene. Atilissuaq at 72˚48.043´N; 55˚54.919´W.*

Figure 62. *Copper-coloured weathering of massive PIC unit on Qaarsorsuaq. View S from Karrat at 72˚50.803´N; 56˚05.343´W.*

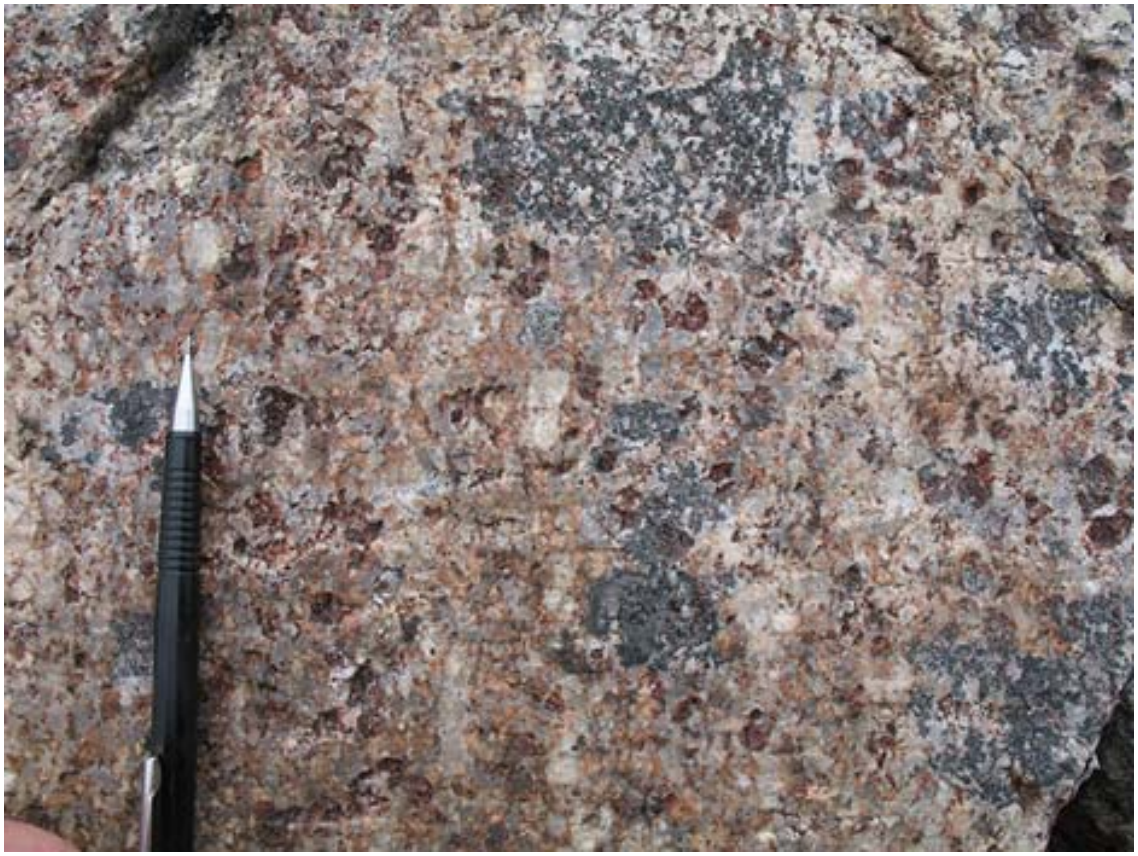

Figure 63. *Magmatic state fabric defined by K-feldspar phenocrysts in charnockite. Atilissuaq at 72˚48.574´N; 55˚55.638´W.*

Close to the contact with paragneiss the PIC contains small enclaves of medium-grained meta-sedimentary rock with a granular texture. These enclaves are interpreted to be metamorphosed greywacke sandstones and meta-pelites. Typical mineral assemblages in the psammitic units include orthopyroxene, plagioclase, quartz and biotite, whereas metapelites consist of garnet, biotite, plagioclase, quartz and spinel. The mineral assemblages are consistent with granulite facies conditions. The charnockite lies structurally above paragneiss with a steep W- to SW-dipping contact parallel to transposed bedding below. Close to the contact, deformation fabric intensity in the PIC and the paragneiss is high, decreasing upward in the PIC. Euhedral to subhedral K-feldspar phenocrysts are observed in exposures with less fabric intensity more than a few 10s of metres above the contact with paragneiss. These are interpreted as incompletely recrystallised phenocrysts and they show an alignment interpreted as a magmatic state fabric, now rotated by deformation parallel to a later crystal-plastic fabric (Figure 63).

Close to the contact with paragneiss, igneous feldspars are completely recrystallised and the charnockite of the PIC contains a strong, planar, crystal-plastic shape fabric defined by quartz and feldspar, and a hypersthene mineral fabric. The charnockite contains leucosome patches flattened sub-parallel to the crystal-plastic shape fabric in the host to define a lithological banding (Figure 59). These leucosomes contain a crystal-plastic planar fabric defined by quartz, feldspar, hypersthene and garnet. Linear shape fabrics (stretching lineations) and kinematic indicators (asymmetrical fabric elements) were observed only in SW Atilissuaq. Here, a stretching lineation in the PIC defined by a hypersthene mineral fabric, and quartz and feldspar shape fabrics, plunges moderately south (Figure 62). Viewed parallel to this lineation (and rotated stereographically to their orientation prior to folding in the Atilissuaq anticline) asymmetric boudins of leucosome bands show transport in this high deformation zone was top-NW (Figure 65).

The lower boundary of the PIC with paragneiss is sharp and distinct (Figure 66). The paragneiss consists of coarse-grained leucosomes of quartz, feldspar, abundant garnet, ± hypersthene in strongly flattened patches parallel to transposed bedding in residual metasandstone units. The rocks are strongly banded and it is likely that the protolith contained thin-bedded sandstone in a siltstone- or shale-dominated sequence (Figure 67).

Planar crystal-plastic fabrics in the paragneiss are defined by quartz and feldspar and at many localities the rock has a weak linear structure defined by an intersection lineation which plunges SW. This is believed to be the intersection between the (weak) axial plane fabric of the Atilissuaq anticline and transposed bedding, comparable to that found in the quartzite. The paragneiss below the main outcrop of the PIC contains relatively thin sheets of charnockite, some of which are folded, and a thick concordant sheet of garnet, quartz, feldspar leucogranite.

Figure 64. *Stretching lineation defined by hypersthene, quartz and feldspar shape fabrics in PIC unit. Atilissuaq at 72˚47.127´N; 55˚55.942´W.*

Figure 65. *Asymmetric boudins of leucosome in PIC. Asymmetry consistent with displacement top-NW. Atilissuaq at 72˚47.127´N; 55˚55.942´W.*

Figure 66. *Contact of PIC with paragneiss. Atilissuaq at 72˚48.044´N; 55˚54.905´W.*

Figure 67. *Paragneiss. Garnet rich leucosome and transposed bedding defined by restitic sandstone units. Atilissuaq at 72˚48.044´N; 55˚54.905´W.*

Aappilattoq-Qassersuaq:

Helicopter reconnaissance field work along the northern margin of the PIC included short ground stops at Aappilattoq (72˚51.959´N; 55˚53.756´W) and northern Qassersuaq (73˚11.438´N; 55˚17.888´W). At Aappilattoq, coarse, hypersthene granite with 1-2 cm K-feldspar phenocrysts contains many rounded enclaves of meta-sedimentary rock (Figure 68). The enclaves consist of quartz, feldspar and relict orthopyroxene. The charnockite has a course granular texture and is dominantly without a deformation fabric apart from a weak crystal-plastic fabric in quartz in some exposures. The enclaves are meta-sandstone or meta-graywacke with bedding truncated by the intrusion but there is no evidence of an early deformation fabric in the meta-sandstone before intrusion of the PIC. The coarse charnockite is cut by a medium-grained, pale grey-weathered hypersthene porphyry sheet or dyke with patches of coarse-grained, hypersthene-quartz-feldspar leucosomes Figure 69).

Figure 68. *Charnockite with meta-sedimentary rock enclave showing bedding. Aappilattoq at 72˚51.959´N; 55˚53.756´W.*

Figure 69. *Medium-grained charnockite sheet or dyke with coarse hypersthene leucosome. Aappilattoq at 72˚51.959´N; 55˚53.756´W.*

On the south coast of the island of Puugutaa, north of Upernavik Isfjord (Ikeq), the NW (lower) contact of the PIC is well-exposed at 72˚51.959´N; 55˚53.756´W. It strikes NE with a moderate dip SE (Figure 1). Meta-sedimentary rocks (migmatitic paragneiss) below the PIC are intruded by concordant sheets of leucogranite. Where individual sheets can be resolved at a metre-scale, they show isoclinal folds with strong boundinage of fold limbs. Fold axial planes are parallel to intense fabric defined by transposed bedding in the meta-sedimentary rocks (Figure 70). Between screens of paragneiss, metre-scale sheets coalesce to form homogeneous leucogranite tabular intrusions exceeding 1km in thickness. Most leucogranite sheets are concordant and strongly deformed although there are some discordant, weakly deformed sheets which imply that emplacement of the leucogranite was syn- to post-tectonic. The zone of high fabric intensity at the base of the PIC extends across strike to the NW for 20 km. It was recognised as a high-strain zone by Escher & Stecher (1978) and called the Tuvssâq (Tussaaq) straight belt. The straight belt extends from the eponymous village NE for >55 km before it is overlain by inland ice. Near the ice, an exposure at 73˚11.438´N; 55˚17.888´W, was in high-temperature porphyroclastic mylonite (Figure 71), so the straight belt is interpreted as a ductile shear zone. NE-trending mylonitic foliation dips 25˚SW with a down-dip stretching fabric defined by deformed leucosome in garnet-biotite schists composed of garnet, biotite, plagioclase, quartz and ilmenite. Asymmetric garnet porphyroclast systems show transport direction was top-NW. In the hanging wall of the shear zone, in the cliffs below Issumaarsuaq, a leucocratic granite sheet and a massive brown-weathered intrusion appear to be folded in a km-scale recumbent isocline (fold nappe) at the base of the PIC.

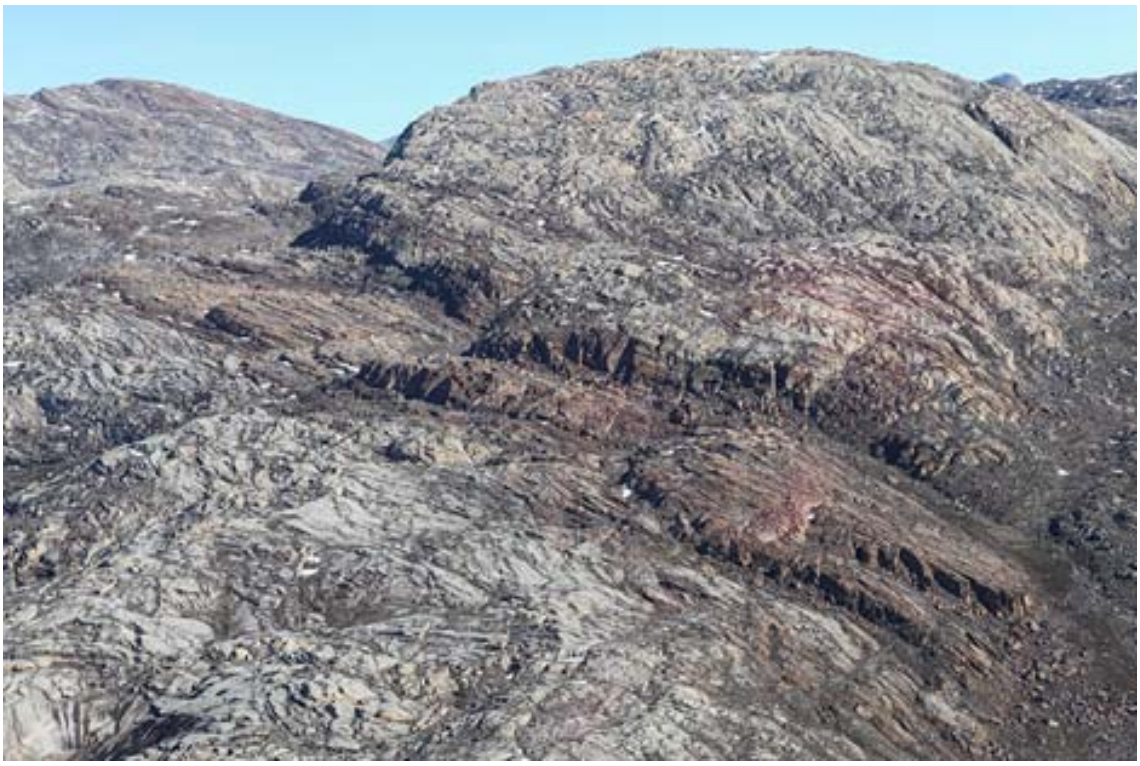

Figure 70. *Zone with high fabric intensity in paragneiss which have been cut by sheets of leucocratic granite below the lower contact with the PIC. S coast Puugutaa, NW of Upernavik Isfjord (Ikeq) at 72˚58´N; 55˚36´W.*

Figure 71. *High-temperature porphyroclastic mylonite, Tuvssâq (Tusssaaq) Straight Belt. Looking W, on surface parallel to down-dip stretching fabric, asymmetry of garnet-quartz-feldspar porphyroclasts shows top-NW displacement. NW of Upernavik Isfjord (Ikeq) at 73˚11.438´N; 55˚17.888´W.*

Karrat (72˚50.803´N; 56˚05.343´W):
The island Karrat to the NW of Atilissuaq island (Figure 1) is composed of migmatitic paragneiss, charnockite of the PIC and a number of leucogranite sheets that are either parallel to or crosscut the foliation at a high angle. Away from the contact with the PIC, the migmatitic paragneiss has a strong layering that is defined by compositional and grain size variations. The rock mainly consists of garnet, biotite, plagioclase, ilmenite and quartz with minor pyroxene, and the mineral assemblage is texturally well equilibrated with the leucosomes. The latter typically occur as melt patches or veins that have irregular contacts with their surroundings, indicative of in situ partial melting. The mineral assemblage in the leucosomes is quartz, plagioclase and garnet. Locally, the migmatitic paragneiss is crosscut by late-tectonic, garnet-bearing granite.

Towards the contact with the PIC, the abundance of leucosomes increases, obscuring the foliation to a degree where the foliation is only defined by an alignment of restitic paragneiss enclaves within a felsic igneous rock. Here, the leucosomes again mainly contain garnet in addition to quartz and plagioclase, although locally, pyroxene and minor biotite have been recorded. The contact between the migmatitic paragneiss and the PIC is marked by the presence of foliation-parallel granite sheets, which appear to be more abundant than further away from the contact (Figure 72). The contact between these leucogranite sheets and the migmatitic paragneiss is diffuse, pointing to a syn-peak emplacement. The migmatitic paragneiss mainly contains garnet, cordierite, biotite, quartz, plagioclase, ilmenite and locally orthopyroxene (Figures 73; 74). The PIC charnockite is a relatively dark, foliated gneiss with a mineral assemblage of orthopyroxene, garnet, plagioclase, ilmenite and quartz that locally contains feldspar phenocrysts. The charnockite is migmatitic with abundant garnetiferous leucosomes. The leucogranite sheets also contain abundant garnet, which is also distinctly larger than in leucogranite further away from the contact. The high modal amount of garnet in the leucogranite sheets indicates that large proportions of the melt were removed prior to final crystallisation.

In the central part of the island, a *c.*1.5-2 km-thick unit of the PIC is located above migmatitic paragneiss with a unit of leucogranite emplaced at the contact (Figure 72). In the paragneiss the degree of partial melting is very high. The rock consists of garnet and hypersthene-bearing leucosomes and residual meta-sandstone units which define transposed bedding (Figure 73). Some leucosomes contain beautiful blue cordierite (Figure 74). Bedding has been transposed to N-striking, steeply E-dipping differentiated layering parallel to flattened leucosomes and a rather weak planar shape fabric defined by feldspar and quartz. This gives an obvious planar fabric to the rock but exposures are rather massive making observation of any linear structure difficult. However, rare asymmetric kinematic indictors are consistent with top-N transport on the main fabric.

Figure 72. *Brown-weathered paragneiss, in the middle-distance,exposed below a sheet of leucocratic granite emplaced at the contact between paragneiss and the PIC (dark exposure in the middle distance above the granite). On Karrat. View SE from near 72˚50.803´N; 56˚05.343´W.*

Figure 73. *Migmatitic, weathered paragneiss. Garnet-hypersthene leucosomes flattened parallel to transposed bedding defined by restitic sandstone. Karrat at72˚50.886´N; 56˚05.295´W.*

Figure 74. *Cordierite-garnet assemblage in leucosome in paragneiss. Karrat at 72˚50.617´N; 56˚04.563´W.*

The lowest leucogranite sheet is slightly discordant and rather poorly defined with diffuse contacts implying that it was melt at the same time as the migmatite (Figure 75). Most of the leucogranite outcrop consists of m- to 10m-thick garnet leucosomes with slightly irregular and diffuse contacts and narrow screens of brown-weathered, slightly wispy, migmatitic paragneiss. The rock is strongly layered and contains a moderately strong crystal-plastic planar shape fabric defined by quartz and feldspar. On foliation surfaces there is a weak S-plunging stretching fabric (linear element of the shape fabric) and slightly asymmetric foliation boudins are consistent with top-N- or NW transport. Toward the top of the sheet enclaves of PIC are present in leucogranite. The enclaves have diffuse contacts implying that the leucogranite was emplaced at the same time as partial melting of the PIC. Enclaves contain partially recrystallised lath-shaped phenocrysts of K-feldspar and a crystal-plastic quartz, feldspar (shape) fabric. In some cases this fabric is truncated against the leucogranite (Figure 76). The contact with the PIC above the sheeted leucogranite unit is sharp. Here, the PIC is a medium- to coarse-grained charnockite containing leucosomes which, near the contact with the leucogranite, contain very large (10 cm) garnet and hypersthene crystals. Leucosomes have been flattened in the plane of a crystal-plastic deformation foliation and this gives the intrusion a banded appearance (Figure 77). In some exposures feldspar phenocrysts define a magmatic state planar fabric although the feldspar laths are recrystallised at the edges and lie parallel with a quartz, feldspar crystal-plastic fabric (Figure 78).

Figure 75. *Paragneiss with leucosome arranged to form sheets with diffuse edges. Increase in the proportion of leucosome leads to the formation of thick leucocratic granite sheets. Karrat, near 72˚50.617´N; 56˚04.563´W.*

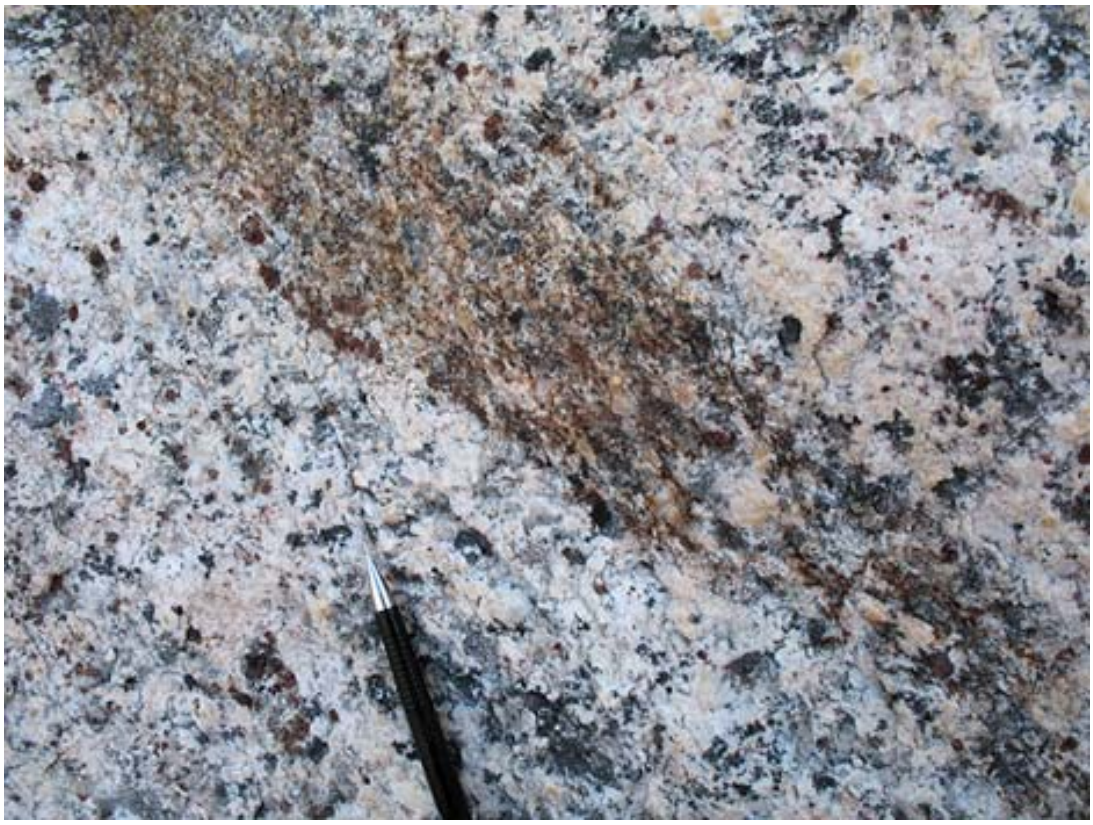

Figure 76. *Leucocratic granite with inclusion of charnockite. Deformation fabric in the charnockite is truncated against the leucogranite. Karrat, near 72˚50.617´N; 56˚04.563´W.*

Figure 77. *PIC with leucosome flattened in the plane of a crystal-plastic deformation fabric to form layering. Karrat, near 72˚50.617´N; 56˚04.563´W.*

Figure 78. *PIC with partially recrystallised feldspar phenocrysts about 2 cm diameter interpreted as phenocrysts in a matrix with a crystal-plastic deformation fabric. Karrat, near 72˚50.617´N; 56˚04.563´W.*

Summary

The Prøven Igneous Complex (PIC) was emplaced as one or more tabular intrusions of a megacrystic granite and deformed subsequently at granulite facies conditions above a high-temperature shear zone. High proportions of partial melting in paragneiss below the complex lead to the generation and emplacement of large volumes of leucogranite just below the PIC.

The northern margin of the PIC is characterised by ductile deformation and partial melting at granulite facies conditions within the complex and within underlying Paleoproterozoic paragneiss and Archean orthogneiss, as established by Rosa et al (2017). The deformation fabric is continuous across the boundary from the PIC into paragneiss and seems to have been formed by the same event in all the rock units.

Toward the inland ice, the zone of intense fabric development in paragneiss below the PIC trends NE and dips SE. At the locality visited (73˚11.438´N; 55˚17.888´W), it is a *c.*20 km-wide (*c.*14 km-thick) zone of high-temperature ductile deformation in paragneiss with (locally) porphyroclastic mylonite, and a down-dip stretching lineation and top-NW displacement. It was recognised and named the Tuvssâq straight belt by Escher and Stecher (1978), renamed as Tussaaq shear zone by Rosa et al. (2017). Near Upernavik, the straight belt and the PIC have been folded by large-scale, close to tight, upright, dome- and basin-like folds (e.g. Atilissuaq anticline).

High grade paragneiss below the PIC has a high proportion of leucosome and was intruded by abundant leucocratic garnet-granite sheets and veins ranging from a few cm to 1 km in thickness. Leucocratic granites are syn- to post tectonic and are most abundant close to the PIC lower contact. They were probably derived by coalescence of leucosomes, melt extraction and migration to form granite sheets. Their concentration just below the PIC may be because of high fluid pressure developed below a cap of charnockite during partial melting.

At the base of the PIC, there is a relatively narrow zone of intense fabric development with complete overprinting of igneous textures where the intrusion was metamorphosed and recrystallised at granulite facies with limited partial melting (metamorphic charnockite). It contains crystal-plastic deformation fabrics defined by feldspar, quartz and hypersthene (with garnet mainly developed in leucosomes) which dip parallel to the lower contact and have a (weak) down-dip stretching lineation.

More than a few 10s of metres above the base of the PIC, crystal-plastic fabrics have not completely overprinted original magmatic fabrics and partially recrystallised, large K-feldspar phenocrysts are preserved.

At 100 m or more above the lower contact, the PIC is typically massive (relatively few joints), has copper-coloured weathering and a greenish colour on fresh broken surfaces. Aligned large feldspar phenocrysts and hypersthene are considered to be part of the magmatic state fabric of the PIC.

The PIC contains enclaves of metasedimentary rocks – mainly sandstone – presumably derived from sedimentary rocks into which it was emplaced. Enclaves contain bedding but do not appear to contain deformation fabrics, even though their mineral assemblages are at granulite facies grades. Nowhere was the PIC seen to intrude already foliated rocks. Post-PIC overprinting means that we were not able to determine whether the host meta-sedimentary rocks were deformed prior to emplacement of the PIC.

The PIC is located at or close to the contact between Archaean gneiss and Paleoproterozoic sedimentary rocks near Upernavik but crops out well within the sedimentary sequence near the inland ice. It may have been thrust into this position from a deeper level. However, present-day erosion is more-or-less at the basement cover contact, and the charnockite must have acquired its sedimentary rock enclaves during intrusion into the sedimentary sequence. This implies that the PIC was intruded into the sedimentary sequence, rather than being thrust into this position after it had originally been emplaced in the deeper crust within Archean basement rocks.

Conclusions

The field relations described in this report demonstrate that the PIC was emplaced close to the basement-cover contact and subsequently displaced to the NW during a major phase of high temperature metamorphism and intense deformation in the Rinkian Orogen (see also Rosa et al. 2017). This conclusion is consistent with recent published geochronological results (Sanborn-Barrie et al. 2017). The published interpretation that the PIC was emplaced late during Rinkian orogenic evolution is rejected (Grocott & Pulvertaft, 1990 and references therein).

Displacement of the PIC to the NW along a high-temperature ductile shear zone was accompanied by: i) granulite facies metamorphism; ii) extensive partial melting in the metasedimentary sequence that formed the host rocks to the PIC; iii) partial melting of the margins of the PIC and iv) emplacement of syn- to post-tectonic leucogranite sheets derived by partial melting of sedimentary rocks below the PIC.

Metamorphism

To the south of the granulite facies PIC, the metamorphic grade in the volcano-sedimentary units of the Karrat Group generally varies between greenschist and amphibolite facies conditions. Granulite facies assemblages are only locally preserved in the Archean basement, whereas the lowest metamorphic grades occur in the Nûkavsak Formation. While this may imply a generally simple stratigraphic control on metamorphic isograds, the amphibolite to granulite facies metamorphism in the Archean basement appears to be mainly Archean in age, whereas the age of metamorphism in the volcano-sedimentary units of the Karrat Group is generally poorly defined as Paleoproterozoic.

The lowermost formation of the Karrat Group (the Qeqertarssuaq Formation) is mainly exposed in the central part of the study area where it consists of quartzite, mica schist and locally garnet-bearing amphibolite. A zircon rim age from a quartzose psammite from this unit was dated at ca. 1822 Ma (Sanborn-Barrie et al. 2017). The Qeqertarssuaq Formation is variably overlain either by the Kangilleq or the Nûkavsak formation. Magmatic apatite from a meta-volcanic rock of the Kangilleq Formation has a U-Pb resetting age of 1826 ± 9 Ma, whereas titanite from the same rock has been dated at 1768 ± 8 Ma (Kirkland et al. 2017).

At the localities visited in 2017, the contacts between the Archean basement, the Qeqertarssuaq Formation and the overlying Nûkavsak Formation are tectonic and no primary depositional features are preserved. Sheets of Archean orthogneiss are intercalated with thin units of quartzite or amphibolite of the Qeqertarssuaq Formation and metapsammite of the Nûkavsak Formation, or are intercalated with amphibolite. Because the amphibolites of the Qeqertarssuaq Formation are always in contact with Archean orthogneiss, it is unclear whether they are Archean or Proterozoic in age. The amphibolites typically consist of hornblende, plagioclase, and quartz ± biotite ± garnet ± clinopyroxene. This assemblage is locally replaced by epidote, zoisite and titanite ± calcite. The mineralogy of the mica schists is generally more complex due to a multitude of metamorphic minerals. Typical amphibolite facies mineral assemblages are garnet-biotite-quartz-plagioclase-alumosilicate (kyanite/sillimanite) ± ilmenite ± tourmaline, whereas lower grade assemblages are quartz-biotite-muscovite-orthoamphibole ± chlorite ± andalusite. Thus, the amphibolites and mica schist of the Qeqertarssuaq Formation appear to share a common metamorphic history that distinguishes them (or the Qeqertarssuaq Formation as a whole) from the overlying formations of the Karrat Group. The local presence of garnet in the amphibolites and kyanite in the mica schists indicates higher pressure conditions early in their metamorphic history that was followed by retrograde greenschist facies metamorphism during, or following, the juxtaposition of this formation with the overlying sequences.

The meta-sedimentary rocks at the base of the Nûkavsak Formation are mainly metapsammitic and locally meta-pelitic rocks that are typically developed as biotite-quartz-plagioclase schist or gneiss, with minor amounts of K-feldspar, ilmenite, and texturally late chlorite and muscovite. The rocks contain abundant quartz veins and are locally silicified. At some localities (e.g., along the north coast of Upernivik Island and on Karrat Island), the

biotite-quartz-plagioclase schists locally contain garnet, sillimanite and/or cordierite. In other localities, porphyroblasts of cordierite and/or andalusite have been documented, e.g. in Svartenhuk. In contrast, the meta-sedimentary rocks at the base of the Nûkavsak Formation in the RTZ Discovery area are very fine-grained and best described as phyllites, characterised by a lower greenschist facies mineral assemblage of muscovite, chlorite, quartz and plagioclase. Further complicating this picture is the fact that rare kyanite-bearing meta-pelitic rocks have also been recorded in the Nûkavsak Formation (Henderson and Pulvertaft, 1987). Thus, the base of the Nûkavsak Formation is characterised by distinct metamorphic field gradients, as has also been reported by e.g. Grocott and McCaffrey (2017).

Structural Geology

During the 2017 field season, we had the opportunity to test some hypotheses: while some of these were discarded, others were confirmed or slightly modified. The new information achieved after the field season combined with the previous two field campaigns give light to a new interpretation of the structural evolution of the Rinkian Orogen. Understanding the structural evolution is intimately related to the understanding of the stratigraphic setting and to the metamorphic history. The new observations, structural data, field mapping, 3D-photogeology and the large amount of analytical data (geochemistry, petrography, zircon dating) collected after three field seasons added new insights that deeply changed the knowledge of the area.

As discussed in the Stratigraphy section, the Qeqertarssuaq Formation was not dated by Henderson and Pulvertaft (1987) and it was assumed to be of Paleoproterozoic age. In the type locality (Qeqertarssuaq), a <50 m-thick package with quartzites sitting above Archean gneiss and below a thick amphibolite (Figure 79) represents the only Paleoproterozoic zircons-bearing quartzite identified to date (Sanborn-Barrie et al. 2017). However, the sequence is repeated tectonically and the stratigraphic relationships are difficult to reconstruct due to the infolding between hornblende-schists, amphibolites, micaschists, quartzites and Archean gneiss (Figures 79 and 80).

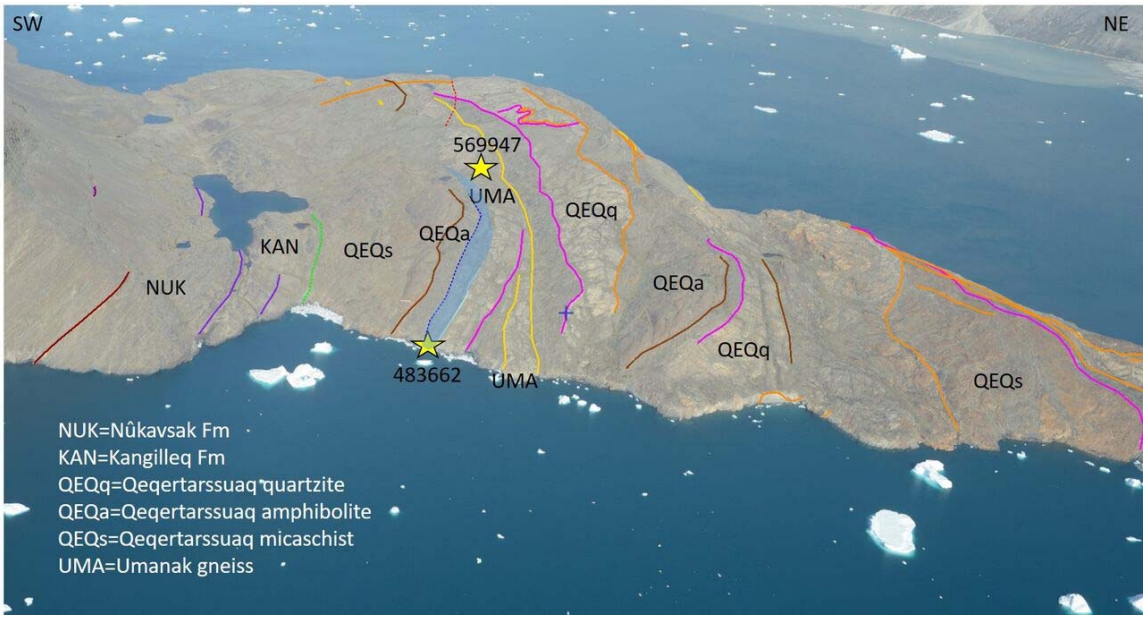

Figure 79. *Oblique photo of the northeastern tip of Qeqertarssuaq Island seen from SE showing the geological boundaries mapped in the 3D-photolab. Sample 569947, previously mapped as quartzites resulted to be Archean gneiss; sample 483662 (Sanborn-Barrie et al. 2017) represents a thin quartzitic layer that could mark the separation between two tectonic units of folded supracrustal rocks.*

The setting resembles other localities where Archean gneiss and Qeqertarssuaq quartzites are in-folded or stacked tectonically. On the other side of the fjord, at less than 2 km in the Kussinersuaq ridge, below a thrust contact with Archean gneiss and quartzites, a thin layer of quartzites, shales and marbles (Qaarsukassak Formation) sits on top of Archean gneiss. Therefore, the thin layer of - Paleoproterozoic zircon-bearing quartzites at Qeqertarssuaq island can be tentatively interpreted as corresponding to the Qaarsukassaq Formation.

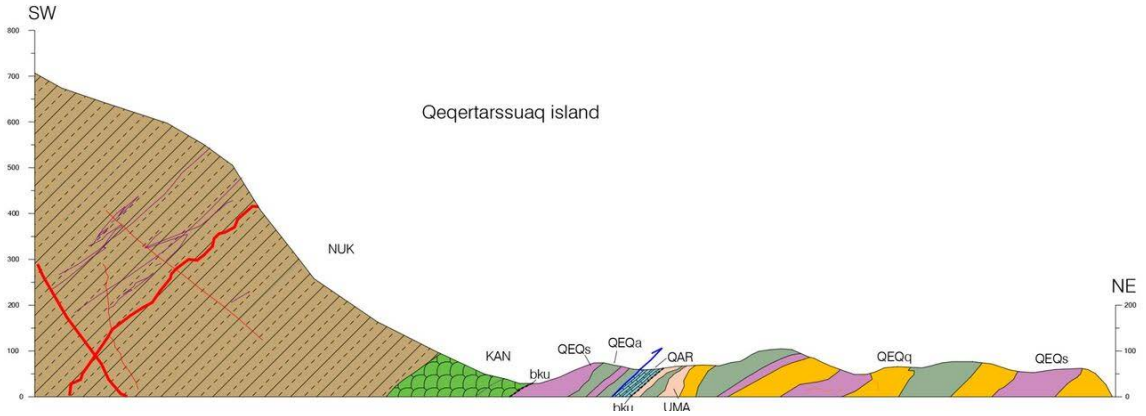

Figure 80. *Geologic cross-section of the northeastern tip of Qeqertarssuaq from 3D-photogrammetry (see the legend in Figure 79).*

In the previous reports (Rosa et al. 2016; 2017), we introduced three main stages of deformation of the Rinkian Orogeny. In the present report we still consider three main stages of Paleoproterozoic deformation and we modify the term Qeqertarssuaq stage because of the unconfirmed stratigraphic age of the Qeqertarssuaq Fm.

The three main deformation stages that affected the Paleoproterozoic Karrat Group can be interpreted as the interference of two orogenic systems, the Rinkian (D1) showing thin-skinned tectonics and HT-metamorphism, and the Nagsugtoqidian (D2-D3) characterised by thick-skinned tectonics. Alternatively it could be the result of interference within the same Rinkian Orogeny with non-coaxial deformation and are distinguished as follows:

- D1 = compressional tectonics, thin-skinned fold-and-thrust belt; E to SE tectonic transport.
- D2 = compressional tectonics, Kigarsima Stage; NNE to NE tectonic transport.
- D3 = compressional tectonics, Maarmorilik Stage; SE tectonic transport.

In the Karrat area, the Paleoproterozoic metamorphism shows a general increase northward and westward, from greenschist facies in Maarmorilik up to granulite facies north of Pannertooq. From the fabrics, the metamorphic conditions and relative timing to granite/pegmatite emplacement, the NW-vergent deformation North of the PIC seems to be contemporaneous with the E to ESE vergent deformation in the southern area. The syn-kinematic granites dated ca. 1830 Ma probably establish the onset of the deformation and age of the metamorphic peak overlapping the reset of apatite at ca. 1826 Ma (Kirkland et al. 2017). North of the Ukkusissat Fjord, the PIC is in tectonic contact with garnet-paragneiss along the Ilulialissuaq Shear Zone (Fig. 82). The kinematics of the reverse shear zone is top-to E or SE (cf. Rosa et al. 2016 Fig. 74). The garnet-paragneiss described earlier, shows evidence of partial melting and is intruded by granite sheets. This sequence is interpreted to represent the high-grade metamorphic equivalent to the Nûkavsak Formation in the south. The Archean orthogneiss and the quartzite, possibly

belonging to the Qeqertarssuaq Formation in Pannertooq, are cut by a top-to-E or SE shear zone (Fig. 81) mapped at least in five localities around the “dome” that it is now interpreted as a tectonic window.

Fig. 81. *Top to-SE (left) shear zone as indicated by quartz porphyroclasts in the Nûkavsak Formation in the southern part of the Pannertooq Window (Fig. 83 section b).*

As introduced above, the granite sheets (Qinngua leucogranites) intruding the Archean gneiss and the Paleoproterozoic meta-greywacke in the Ukkusissat Fjord are dated at ca. 1830 Ma and interpreted to be syn-kinematic emplacement during granulite-facies metamorphism in that area.

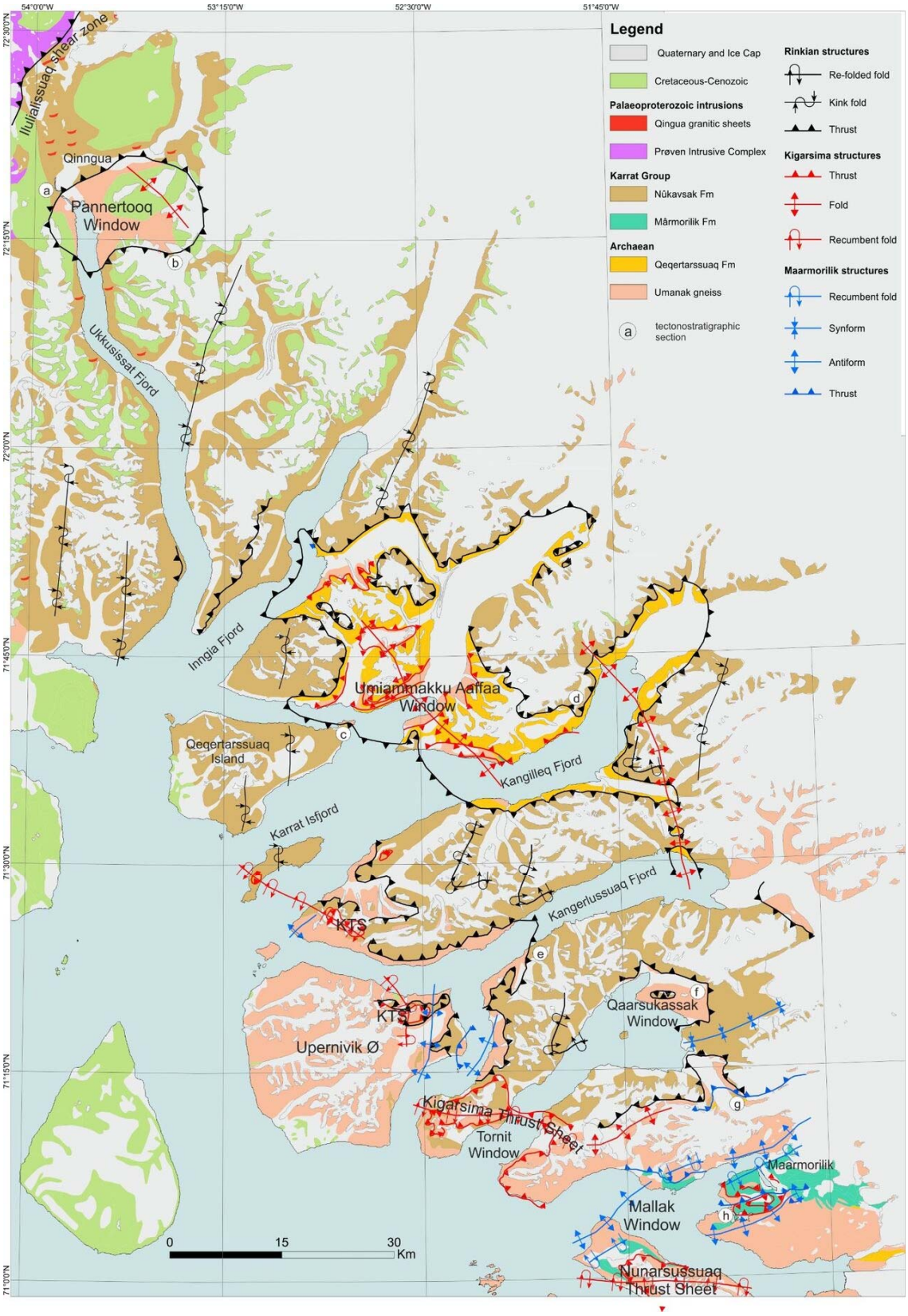

Figure 82. *Structural map of the Karrat area showing the thin-skinned fold-and-thrust belt structures re-folded during thick-skinned tectonics (Kigarsima and Maarmorilik structures).*

The presence of a shear zone near the base of the Nûkavsak and Kangilleq formations was found in many localities within the region. This structural evidence, also noted by Henderson and Pulvertaft (1987), indicates that the “Upper Karrat Group” is detached from the underlying “basement” and the shear zone represents the sole thrust of a fold-and-thrust belt. Since the Archean gneiss is not involved in this stage, we interpret it as evidence for thin-skinned tectonics. The tectonic transport is top-to-E or ESE associated with N-S to NNE-SSW trending isoclinal folds and kink-folds in the Nûkavsak meta-greywacke. We refer to this as the thin-skinned fold-and-thrust belt (FTB, Figure 82 and 83).

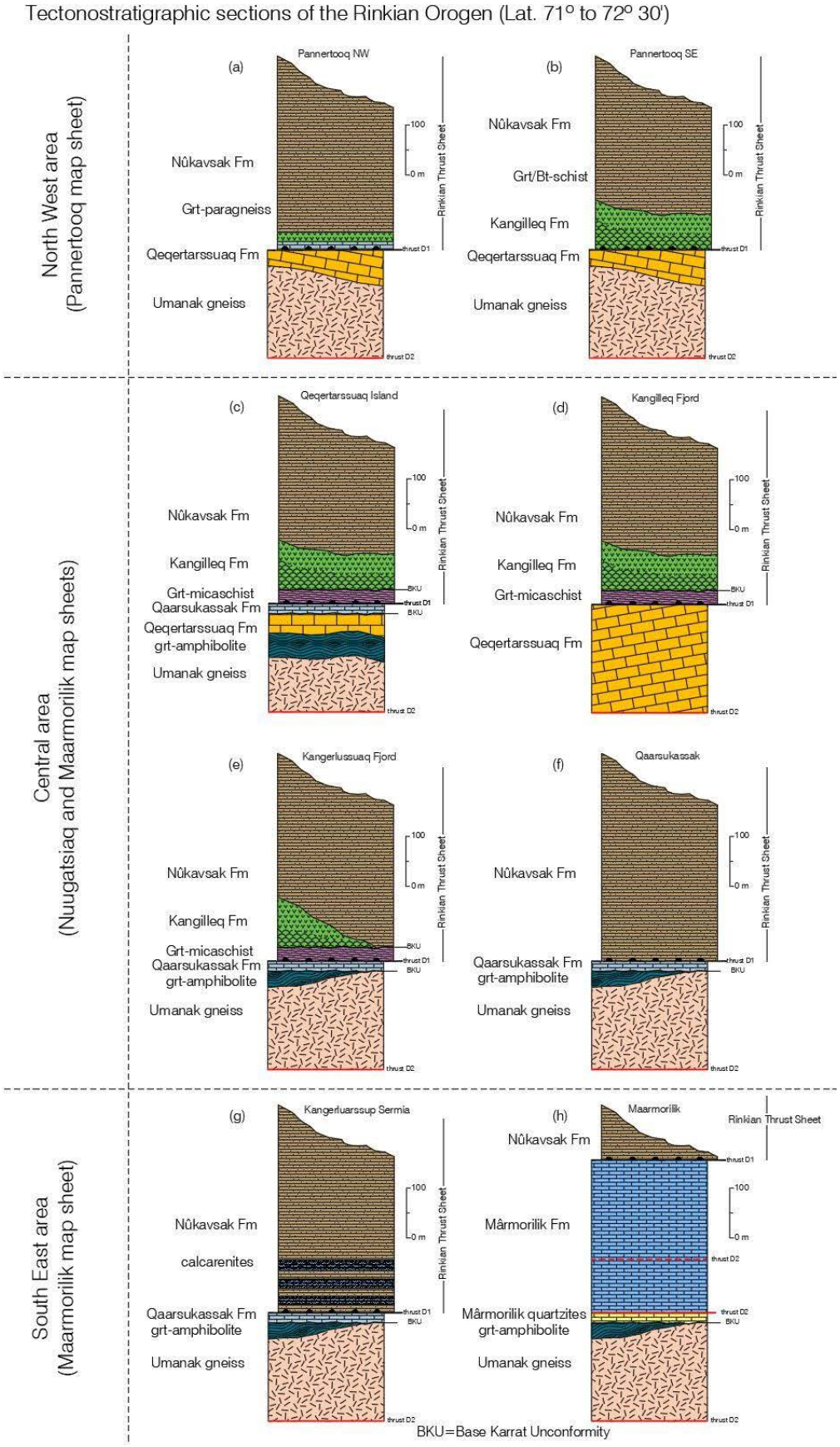

Figure 83. *Tectonostratigraphic sections representing major tectonic units of the Rinkian Orogen in the Karrat area. Circled letters refer to the locations in Figure 80.*

A sand box model is shown as an analogue to the fold-and-thrust system of the Rinkian orogen (Figure 84). In the Rinkian orogen the basal detachment would be located near the base of the Nûkavsak or the Kangilleq formations where, in some cases, a thick layer of garnet-micaschist is preserved in the hangingwall of the sole thrust (Figure 83). The latter micaschist could be either equivalent to the garnet-paragneiss from Pannertooq (Figure 83-a,b) or to the Qeqertarssuaq micaschist. In the central part of the region (Figure 83-c,e), biotite-schist of the Nûkavsak Formation and/or pillow basalts of the Kangilleq Formation lie unconformably on quartzites or garnet-micaschists with staurolite (±sillimanite ±kyanite) belonging to the Qeqertarssuaq Formation. In the footwall of the Rinkian FTB in the central part of the region, below the garnet-micaschist or biotite-schists of the Nûkavsak Formation, it is possible to find a few metres-thick units of quartzite, black shale and marble interpreted as the Qaarsukassak Formation that, in turn, sits unconformably onto garnet-amphibolite (Figure 83-e,g). In the southern area (Figure 83-h), the hangingwall is represented by the Nûkavsak pelites on top of the Mârmorilik marbles representing the footwall.

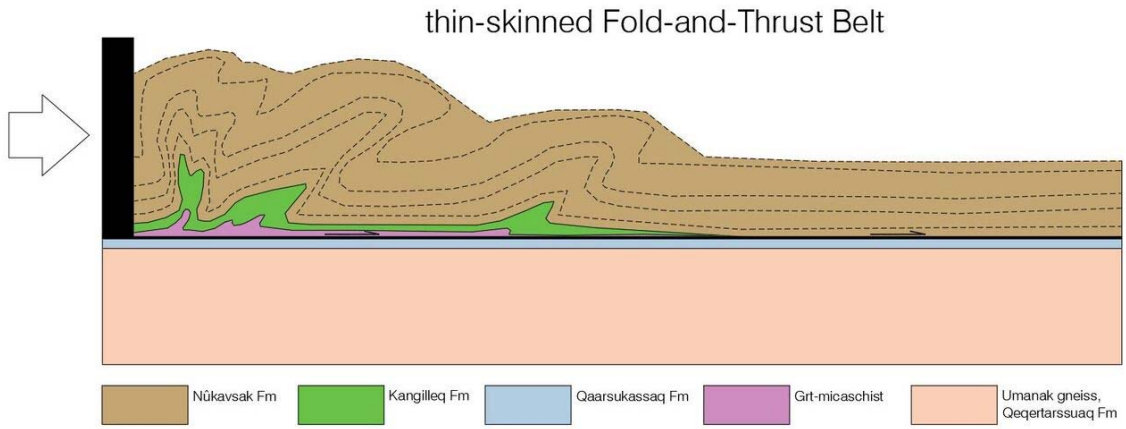

Figure 84. *Sandbox model showing geometries and structures of a fold-and-thrust belt with a 33% of shortening.*

An alternative interpretation of the structural evolution of the Karrat area has been published by Grocott and McCaffrey (2017) who introduced the Karrat Fjord thrust system that was firstly emplaced toward the east and then reworked during top-NW tectonic transport.

The thin-skinned FTB is subsequently re-folded during the Kigarsima and Maarmorilik events. These later events are related to thick-skinned tectonics during which Archean gneiss and supracrustal rocks, form the cores of isoclinally-fold nappes as in Kigarsima and Nunarsussuaq or stacks of thrust sheets as the Kussinerssuaq duplex (Figure 85) in the Ummiammakku Aaffaa tectonic window (Figure 82).

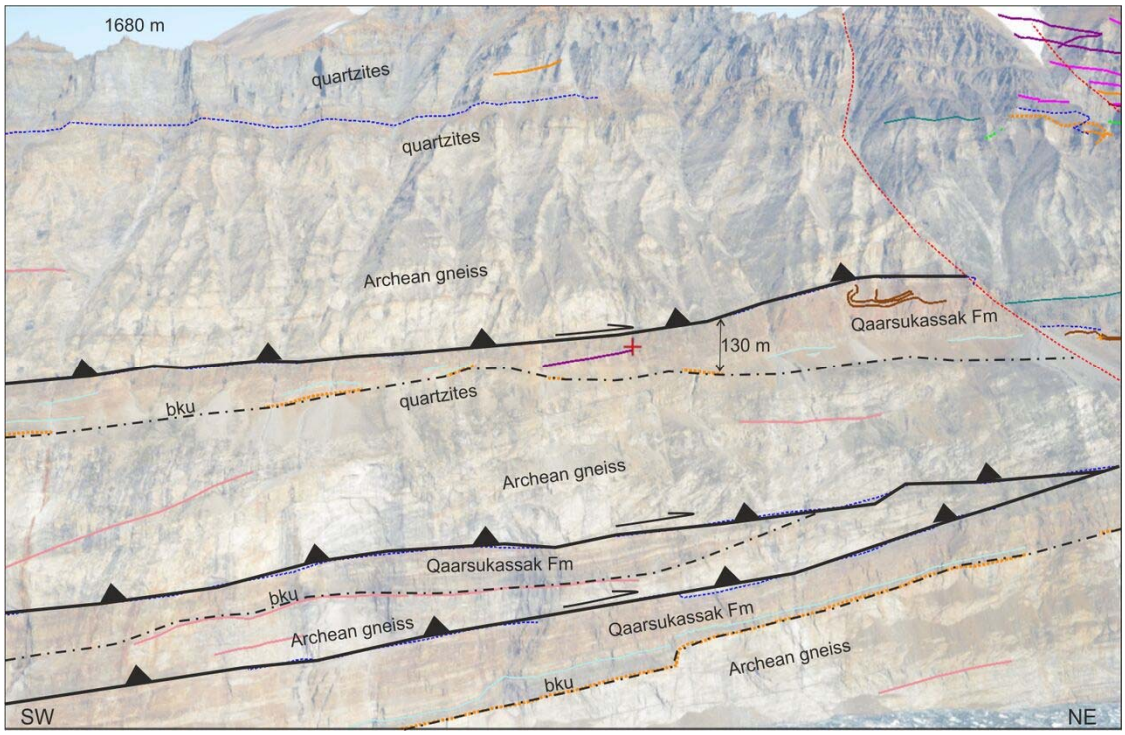

Figure 85. *Oblique photo of the Kussinerssuaq ridge seen from SE. One of the meta-pelite horizons mapped in the 1:100 000 Nuugatsiaq map sheet (Henderson and Pulvertaft, 1987) was visited in 2017 (red cross) and interpreted to be the Qaarsukassaq Formation (see Stratigraphy section). By analogy, other two rusty horizons in the first half of the mountain ridge are interpreted as Qaarsukassak Formation. The structure is interpreted to be a tectonic stack of Archean gneiss and Paleoproterozoic meta-sediments forming the Kussinerssuaq Duplex. Bku=Base Karrat Unconformity.*

One of the key geological features to be tested by using 3D-photogrammetry to unravel the relative chronology and fold interference between D1 and D2 structures is represented by the so-called “overfold” (Henderson and Pulvertaft, 1987) exposed in the northern side of Kangerlussuaq Fjord (Figure 82 “Rinkian refolded folds”). Figure 86-a is a geologic cross-section from the 3D-photogeology of the area showing a monocline structure of Archean gneiss and sheared garnet-micashists dipping toward NNE covered with a deeply folded sequence of meta-greywackes of the Nûkavsak Fm. As firstly described by Henderson & Pulvertaft (1987, figure 36) in this area spectacular examples of refolded kink-folds by a later large overfold is observed. The axial planes of the kink-folds are clearly refolded as shown in the cross-section (Figure 86-a) and visible also in the oblique photo (Figure 86-b).

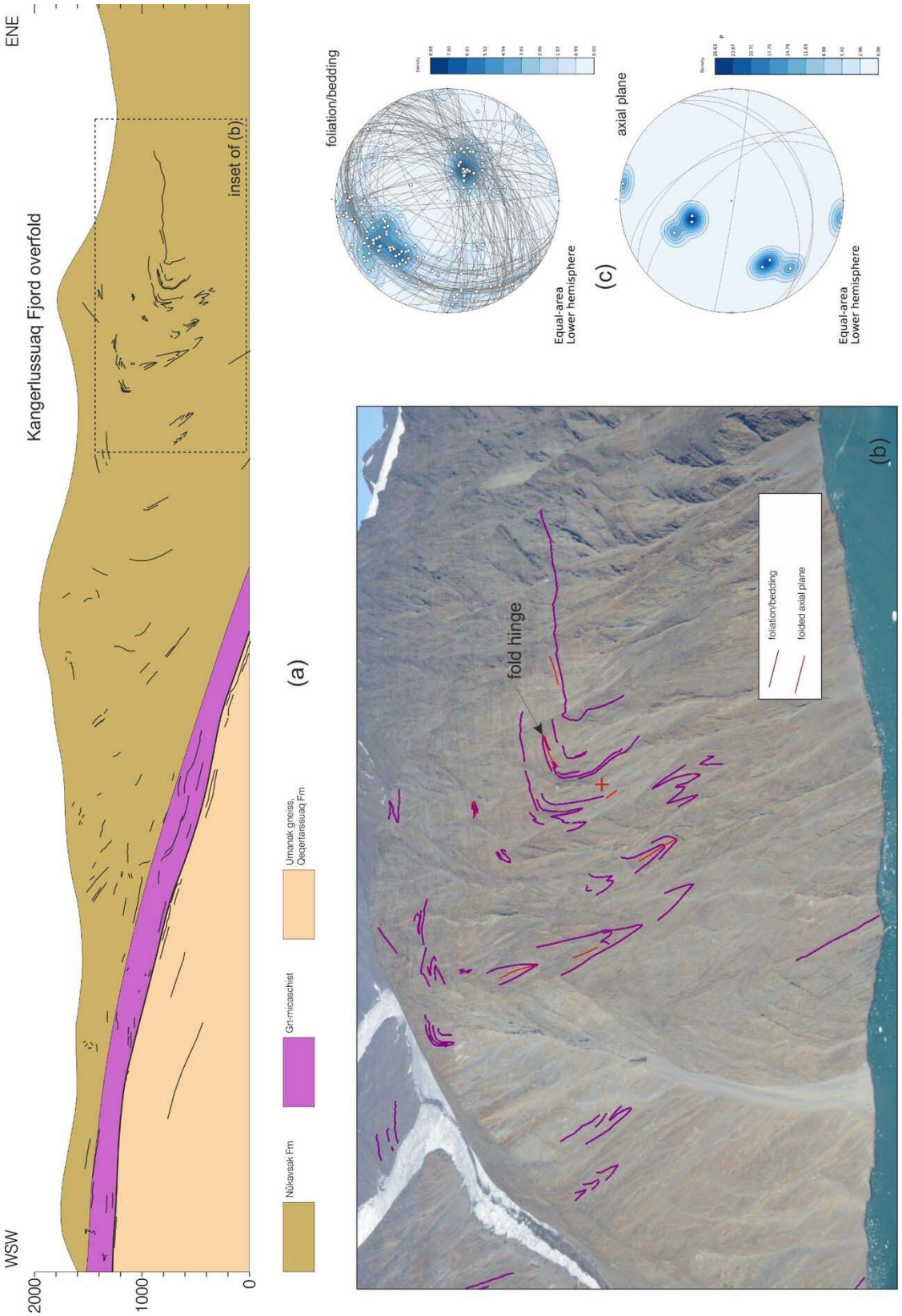

Figure 86. *a) Geologic cross-section of the Kangerlussuaq "overfold"; b) oblique photo of the re-folded kink-folds showing of the results of 3D-mapping; c) Equal area, lower hemisphere stereoplots of the pole to bedding/foliation, great circles and density of Nûkavsak Formation and axial planes of the "overfold".*

The strike-dip measurements (Figure 86-c) obtained from 3D-polylines mapped in the photogrammetry lab at GEUS were separated in two datasets: (1) bedding/foliation of the Nûkavsak Fm and (2) axial planes of the kink-folds. The lower hemisphere equal area stereoplot of the bedding/foliation show a main NE-SW trending fold axis while the stereoplot of the axial planes dataset show a fold axis plunging 30º toward SE. Similar data were obtained from the detailed mapping of the Karrat area (Sørensen and Guarnieri, 2018).

The preliminary conclusion of this structural analysis is that the kink-folds are consistent with a NW-SE to WNW-ESE compression while the “overfold” (the re-folding of the earlier kink-folds) is consistent with a SW-NE compression. The two trends seem to be respectively coherent with D1 and D2. Finally, the SE-plunging of the F2 fold axis (Figure 86-c) could be interpreted as the effect of D3 upright folds.

Economic Geology

With the project aims now focusing on revising map sheets, less efforts were put on prospecting or mineral reconnaissance. Nevertheless, whenever visits were made to newly-identified areas of favourable stratigraphy, zinc zap was applied to sulfate/carbonate encrustations that could be derived from the weathering of primary sulfides.

A suitable stratigraphic host for carbonate-hosted Zn-Pb, the Qaarsukassak Formation, was identified in Kussinersuaq, west of at the mouth of the Umiammakku glacier (see Stratigraphy section), so this locality was briefly visited to look for signs of mineralisation. The sequence of quartzite white/gray tremolitic marble, micaceous chert and/or siliceous schist can be followed laterally for several hundred metres, but was only accessed in a few places. Faint positive zinc zap results were obtained in two localities (Figure 87), in both instances between the marble and the micaceous chert horizon, but it was impossible to trace the results from sulfate encrustations to primary sulfides. Two friable and sulfate/carbonate encrusted chert and marble samples were collected, and one of them yielded a low, yet anomalous, concentration of 0.12% Zn (sample 561243).

The significance of this finding is that this locality is located approximately 50 km NW of the RTZ Discovery showing (Coppard et al, 1992), where the Qaarsukassak Formation was first described (Rosa et al, 2016). This significantly enlarges the extent of this formation and, thereby, of the potential for Zn-Pb mineralisation within.

Figure 87 - *Sulfate encrustations yielding faint positive zinc zap results, between a marble and a micaceous chert horizon at Kussinersuaq.*

Regarding the potential for orogenic gold mineralisation, quartz-pyrite veins surrounded by actinolite-biotite-pyrite hydrothermal alteration, identified within the Nunataq Formation, south of Marmorilik (described in the Archean section), were sampled. Some wider alteration zones consist of silicified bands associated with actinolite-biotite-pyrite (distal) carbonate, epidosite, fuchsite and pyrite schists (proximal), often associated with intense shearing. The alteration zones appear to cut primary lithologies of amphibolites and metasediments. Typically, the alteration zones are 2-5m wide, with a center of epidosite and fuchsite and sporadic mineralisations of pyrite and trace chalcopyrite. The zones dip steeply to the north (ca 50°) with a E-W strike. Four samples were collected from across four of such alteration zones. However, their assays yielded no significant gold values.

Conclusions and recommendations

Significant progress has been made in the 2017 field season, aimed at the revision of the 1:100k geological map sheets of the southern Karrat Group exposures and the underlying Archean (Umanak and Nunataq formations), as well as at the understanding of the role of the PIC in the evolution of the area.

The age and stratigraphic assignment of the Qeqertarssuaq Formation is uncertain, since there is some evidence that this formation registers deformation and metamorphism that predates deposition of the Qaarsukassak Formation and the remaining Karrat Group. Further detrital zircon geochronology should, therefore, be carried out on key samples, to verify whether a Paleoproterozoic zircon-bearing unit can be distinguished from a unit lacking zircon grains with these ages. Since populations of detrital zircon grains also depend on the sediment source areas, the geochronology results should be combined with results of pseudo-sections, which can unravel the metamorphic evolution of different units, as well as with the structural geology observations, to validate whether two formations can be set aside and can consistently be mapped.

Photogeological mapping should attempt to link the Qaarsukassak Formation present at the RTZ Discovery showing (Coppard et al. 1992) to that now identified in Kussinersuaq and in between, to underpin the potential for Zn-Pb mineralisation hosted by this formation and assist in mineral exploration. Integrated 3D hyperspectral data could add mineralogical information to the photogeology results. The combined approach should be further tested and evaluated for the potential of remote mapping techniques. In particular, scenes from the 2016 field campaign from Kangerluarsuk Fjord, Inukassaat Fjord and Kangerlussuaq Fjord should be carefully evaluated for occurrence of Qaarsukassak Fm. Further, interesting scenes would be the coastal scans of Svartenhuk Ø or along Ukkusissat Fjord to map, e.g., thurst repetition or metamorphism related mineralogical changes in the Nûkavsak Fm, or delineate mineralogically different granite sheets around Pannertooq.

The study of the distribution and the physical volcanology of the mafic volcanic rocks of the Kangilleq Formation (informal), focused on horizons with distinct geochemical signatures (alkaline vs. subalkaline), as identified in samples collected in previous seasons, in order to elucidate the petrogenesis of these volcanic rocks. Additional follow-up petrography and detailed lithogeochemistry of the Kangilleq Formation, with samples analyzed for radiogenic isotopes, will assist in constraining the different metavolcanic units within this formation, with particular emphasis on their petrogenesis as this will have an impact on exploration targeting for volcanogenic massive sulfide deposits.

The PIC is now interpreted to have been emplaced, as one or more tabular intrusions, possibly before orogenic deformation and metamorphism, rather than being late syn-tectonic, as traditionally considered. This has significant implications for the understanding of the tectonic evolution of the area.

The main deformation stages that affected the Paleoproterozoic Karrat Group can be interpreted as the interference of two orogenic systems: the Rinkian (D1) showing HT-

metamorphic rocks and the Nagsugtoqidian (D2-D3) characterised with lower grade metamorphism alternatively it could be the result of interference within the same Rinkian Orogeny with non-coaxial deformation and are distinguished as follows:
D1 = compressional tectonics, thin-skinned fold-and-thrust belt; E to SE tectonic transport.
D2 = compressional tectonics, Kigarsima Stage; NNE to NE tectonic transport.
D3 = compressional tectonics, Maarmorilik Stage; SE tectonic transport.

Finally, drone-borne acquisitions using multi-spectral cameras on fixed-wing systems should be used for further reconnaissance mapping in the first stage of fieldwork. They can be a valuable reconnaissance tool for mapping structural and surface alteration indicators.

Acknowledgements

The financial support from the Ministry of Mineral Resources (Greenland) and of GEUS is appreciated. Helmholtz-Zentrum Dresden-Rossendorf is thanked for support with an hyperspectral camera and UAS technology. The authors would also like to acknowledge the excellent working relation with Minna Martek's crew, Poul, Ingut and François, as well as with Air Greenland's helicopter pilot Inge Fast. Finally, fruitful discussions with Jim Connelly, Adam Garde, Julie Hollis, Ty Magee, Crystal Laflamme, Gabriel Unger, and Kristine Thrane are also acknowledged. Crystal Laflamme is also acknowledged for her constructive review of this report.

References

Carmichael A. 1985: Tectonics and Mineralisation of the Black Angel Mine, West Greenland, Department of Earth Sciences, University of London, Goldsmith's College, Report No. 1 (in archives of Geological Survey of Denmark and Greenland, GEUS Report File 20522)

Chilingar, G. V. 1957: Classification of Limestones and Dolomites on basis of Ca/Mg ratio. *Journal of Sedimentary Petrology*, *27*(2), 187–189. https://doi.org/https://doi.org/10.1306/74D7069B-2B21-11D7-8648000102C1865D

Connelly, J.N., Thrane, K., Krawiec, A.W. & Garde, A.A. 2006. Linking the Palaeoproterozoic Nagssugtoqidian and Rinkian orogens through the Disko Bugt region of West Greenland. Journal of the Geological Society, London, 163, 319–335.

Coppard, J., Swatton, S. & Harris, C. J. 1992: Karrat exclusive exploration licence. 1992 year end report. Internal report, RTZ Mining and Exploration Ltd., pp 19 (in archives of Geological Survey of Denmark and Greenland, GEUS Report File 21297).

Escher, A. & Pulvertaft, T.C.R. 1968: The Precambrian rocks of the Upernavik-Kraulshavn area (72˚00´-74˚15´N), West Greenland. Rapport Grønlands Geologiske Undersøgelse 15, 11-14.

Escher, A. & Pulvertaft, T.C.R. 1976: Rinkian mobile belt of West Greenland. In: Escher, A. & Watt, W.S. (eds.) Geology of Greenland, 105-119. Copenhagen: Geological Survey of Greenland.

Escher, J.C. & Stecher, O. 1978: Precambrian geology of the Upernavik-Red Head region (72˚15´-75˚15´N), northern West Greenland. Rapport Grønlands Geologiske Undersøgelse 90, 23-26.

Escher, J.C. & Stecher, O. 1980: Fieldwork on Precambrian granites and metasediments in the Søndre Upernavik-Kuvdlorssuaq region 72˚00´-74˚40´N) northern West Greenland. Rapport Grønlands Geologiske Undersøgelse 100, 38-41.

Garde, A.A., 1978: The Lower Proterozoic Mârmorilik Formation, east of Mârmorilik, West Greenland. Meddelelser om Grønland 200(3), 71 pp

Grasemann, B., Martel, S. and Passchier, C. 2005. Reverse and normal drag along a fault. Journal of Structural Geology, 27(6), 999–1010. doi: 10.1016/j.jsg.2005.04.006.

Grocott, J. & Vissers, R.L.M. 1984: Field mapping of the early Proterozoic Karrat Group on Svartenhuk Halvø, central West Greenland. Geological Survey of Greenland Report, 120, 25-31

Grocott, J. & Pulvertaft, T.C.R. 1990: The Early Proterozoic Rinkian belt of central West Greenland. In: Lewry, J.F. & Stauffer, M.R. (eds) The Early Proterozoic Trans-Hudson orogen of North America. Geological Association of Canada, Special Paper, 37, 443-463.

Grocott, J. & McCaffrey, K.J.W. 2017: Basin evolution and destruction in an Early Proterozoic continental margin: the Rinkian fold-thrust belt of central West Grenland. Journal of the Geological Society, 174, 453-467, 27 January 2017, https://doi.org/10.1144/jgs2016-109

Guarnieri, P.; Partin, C.A. & Rosa, D., 2016: Palaeovalleys at the basal unconformity of the Palaeoproterozoic Karrat Group, West Greenland. Geological Survey of Denmark and Greenland Bulletin 35, 63–66

Henderson, G. & Pulvertaft, T.C.R. 1967: The stratigraphy and structure of the Precambrian rocks of the Umanak area, West Greenland. Meddelelser fra Dansk Geologisk Forening, 17, 1-20.

Henderson, G & Pulvertaft, T.C.R. 1987: Lithostratigraphy and structure of a Lower Proterozoic dome and nappe complex. Geological Survey of Greenland Descriptive text for Geological Map of Greenland 1:100 000-scale sheets Mârmorilik 71 V.2 Syd, Nûgâtsiaq 71 V.2 Nord, Pangnertôq 72 V.2 Syd.

Kalsbeek, F. 1981: The northward extent of the Archean basement of Greenland – a review of Rb-Sr whole-rock ages. Precambrian Research 91, 383-399.

King, A.R., 1981: Report on prospecting and correlation programme, in the Maarmorilik Fomration, West Greenland. Greenex A/S (in archives of the Geological Survey of Denmark and Greenland, GEUS Report File 20419).

Kirkland, C.L. Hollis, J., Danišík, M., Petersen, J., Evans,N.J. & McDonald, B.J., 2017, Apatite and titanite from the Karrat Group, Greenland; implications for charting the thermal evolution of crust from the U-Pb geochronology of common Pb bearing phases, Precambrian Research,300,107-120. https://doi.org/10.1016/j.precamres.2017.07.033.

Lorenz, S., Salehi, S., Kirsch, M., Zimmermann, R., Unger, G., Vest Sørensen, E., & Gloaguen, R. 2018: Radiometric Correction and 3D Integration of Long-Range Ground-Based Hyperspectral Imagery for Mineral Exploration of Vertical Outcrops. *Remote Sensing*, *10*(2), 176. https://doi.org/10.3390/rs10020176

Meer, F. Van Der, Kopackova, V., Koucká, L., Werff, H. M. A. Van Der, Ruitenbeek, F. J. A. & Van and Bakker, W. H. 2018: Wavelength feature mapping as a proxy to mineral chemistry for investigating geologic systems : An example from the Rodalquilar epithermal system. International Journal of Applied Earth Observation and Geoinformation, 64, 237–248. doi: 10.1016/j.jag.2017.09.008.

Pedersen, F. D. 1980: Remobilization of the massive sulfide ore of the black angel mine, central west Greenland. *Economic Geology*, *75*(7), 1022–1041. https://doi.org/10.2113/gsecongeo.75.7.1022

Rosa, D., Guarnieri, P., Hollis, J., Kolb, J., Partin, C., Petersen, J., Sørensen, E.V., Thomassen, B., Thomsen, L & Thrane, K. 2016: Architecture and mineral potential of the

Palaeoproterozoic Karrat group, West Greenland: results of the 2015 season. Danmarks og Grønlands Geologiske Undersøgelse Rapport 2016/12, 98pp

Rosa, D., Dewolfe, M., Guarnieri, P., Kolb, J., LaFlame, C., Partin, C., Salehi, S., Sørensen, E.V., Thaarup, S., Thrane, K. & Zimmermann, R. 2017: Architecture and mineral potential of the Palaeoproterozoic Karrat group, West Greenland: results of the 2016 season. Danmarks og Grønlands Geologiske Undersøgelse Rapport 2017/5, 111pp.

Salehi, S., Lorenz, S., Sørensen, E. V., Zimmermann, R., Fensholt, R., Heincke, B. H., Kirsch, M. & Gloaguen, R. 2018: Integration of Vessel - Based Hyperspectral Scanning and 3D - Photogrammetry for Mobile Mapping of Steep Coastal Cliffs in the Arctic. *Remote Sensing*, *10*, 1–28. https://doi.org/10.3390/rs10020175

Sanborn-Barrie, M., Thrane, K., Wodicka, N & Rayner, N. 2017: The Laurentia-West Greenland connection at 1.9 Ga: new insights from the Rinkian fold belt. Gondwana Research 51, 289-309.

Sørensen, E. V. & Guarnieri, P. 2018: Remote geological mapping using 3D photogrammetry: an example from Karrat, West Greenland. Geological Survey of Denmark and Greenland Bulletin.

Thrane, K., Baker, J., Connelly, J. & Nutman, A. 2005: Age, petrogenesis and metamorphism of the syn-collisional Prøven igneous complex, West Greenland. Contributions to Mineralogy and Petrology, 149, 541-555.

Unger, G. 2018: *3D Integration of multi-source and multi-scale exploration data: The example of the Paleoproterozoic Mârmorilik Pb-Zn- deposit / Central-West Greenland*. Unpubl. M..Sc. thesis, TU Bergakademie Freiberg, 70pp.

Zaini, N., van der Meer, F., & van der Werff, H. 2012: Effect of grain size and mineral mixing on carbonate absorption features in the SWIR and TIR wavelength regions. *Remote Sensing*, *4*(4), 987–1003. https://doi.org/10.3390/rs4040987